Encyclopaedia of Nuclear Energy

Magnetic Confinement Fusion - Development Facilities

A.J.H. Donné[1,2], G. Federici[1], A. Ibarra[3], J. Menard[4], F. Warmer[5]

[1] EUROfusion, Boltzmannstrasse 2, 85748 Garching, Germany
[2] Dutch Institute for Fundamental Energy Research, Eindhoven, The Netherlands
[3] CIEMAT, Avda. Complutense 40, Madrid 28040, Spain
[4] Princeton Plasma Physics Laboratory, Princeton, NJ, USA
[5] Max-Planck Institute for Plasma Physics, Greifswald, D-17491, Germany

Abstract

Roadmaps have been developed to achieve fusion electricity as quickly as possible. All roadmaps have as the central element the construction and exploitation of ITER, which will, for the first time, exhibit a fusion gain of $Q \geq 10$. ITER will test essential technologies that are required for the next step, including tritium breeding, and will demonstrate that fusion is feasible on a scale appropriate to practical exploitation. A variety of ideas are being evaluated for the steps after ITER. Some countries are designing relatively large demonstration plants that are based on an extrapolation from ITER, thereby using proven technologies as much as possible. Japan, Korea and the EU have labeled their devices JA-DEMO, K-DEMO and EU-DEMO, while China is working on the Chinese Fusion Experimental Test Reactor. The USA and the UK are focusing their activities on smaller devices based on the spherical tokamak, and a similar approach is followed by a number of privately funded enterprises that focus on spherical tokamaks featuring high-field superconductors. Conceptual studies of stellarator-based fusion power plants are also being conducted in Europe and Japan. Since materials in future devices will experience much higher neutron loads than in ITER, new materials must be developed or the operational space of existing materials must be expanded. It is critical, therefore, that the materials are tested and validated in a dedicated neutron source exhibiting a similar spectrum to that in a fusion reactor. The most prominent of these (accelerator-based) facilities are IFMIF/DONES in Europe and A-FNS in Japan. Some countries focus also on volumetric neutron sources based on plasma devices. This chapter will give an overview of the major development devices within the magnetic confinement fusion program. It also includes a brief description of several non-nuclear devices that are currently being constructed and that will give support to the main line of nuclear fusion devices.

Keyword: Nuclear fusion, ITER, Demonstration reactor, neutron sources

Glossary

Beta normalized	Operational parameter indicating how close the plasma is to reaching the Greenwald density limit or a destabilizing major magneto-hydrodynamic instability
Bootstrap current	A self-generated current due to collisions between trapped and passing plasma particles. The bootstrap fraction is strongly influenced by the density gradient
DCLL	Dual-Coolant Lithium Lead– one of the possible concepts for the tritium breeding blanket
Disruption	In a disruption the plasma confinement is lost in milliseconds. Often this occurs after a vertical displacement event of the plasma column or after the growth of non-axisymmetric magneto-hydrodynamic instabilities
ECRH	Electron Cyclotron Resonant Heating
Edge Localised Mode (ELM)	Disruptive instability in the plasma edge region due to a quasi-periodic relaxation of the edge transport barrier formed during the transition from low (L) to high (H) confinement mode.
Greenwald scaling	Empirical upper limit for the central line-averaged density which depends on plasma current and minor radius
HCCB	Helium-Cooled Ceramic Breeder – one of the possible concepts for the tritium breeding blanket
HCLL	Helium-Cooled Lithium Lead– one of the possible concepts for the tritium breeding blanket
HCPB	Helium-Cooled Pebble Bed – one of the possible concepts for the tritium breeding blanket
HTSC	High-Temperature Superconductor
ICRF	Ion Cyclotron Radiofrequency Heating
IFMIF/DONES	International Fusion Materials Irradiation Facility / DEMO Oriented Neutron Source
IFMIF/EVEDA	International Fusion Materials Irradiation Facility / Engineering Validation and Engineering Design Activities
LHH	Lower Hybrid Heating
LTSC	Low-Temperature Superconductor
Martin scaling	Empirical scaling for the power required to access the H-mode
NBH	Neutral Beam Heating
Snowflake divertor	A divertor geometry that effectively spreads the heat load from the plasma over four instead of over two footprints, thereby effectively lowering the heat load on the divertor materials
WCLL	Water-Cooled Lithium Lead– one of the possible concepts for the tritium breeding blanket

1. Introduction- the path towards fusion electricity

A number of countries have developed fusion roadmaps or strategic plans, in order to clarify which steps need to be taken to achieve electricity generation from fusion (Donné et al., 2018; Okano, 2019; Wan et al., 2017; National Academy of Sciences, 2019). Although there are differences between the various fusion roadmaps, there are also many commonalities, which are depicted in Figure 1. All roadmaps include ITER (Bigot, 2019) as an essential step. ITER will demonstrate that energy from fusion is feasible by aiming at a plasma power multiplication ($Q = P_{fusion}/P_{in}$) of 10 and it will demonstrate essential fusion technologies, such as tritium breeding.

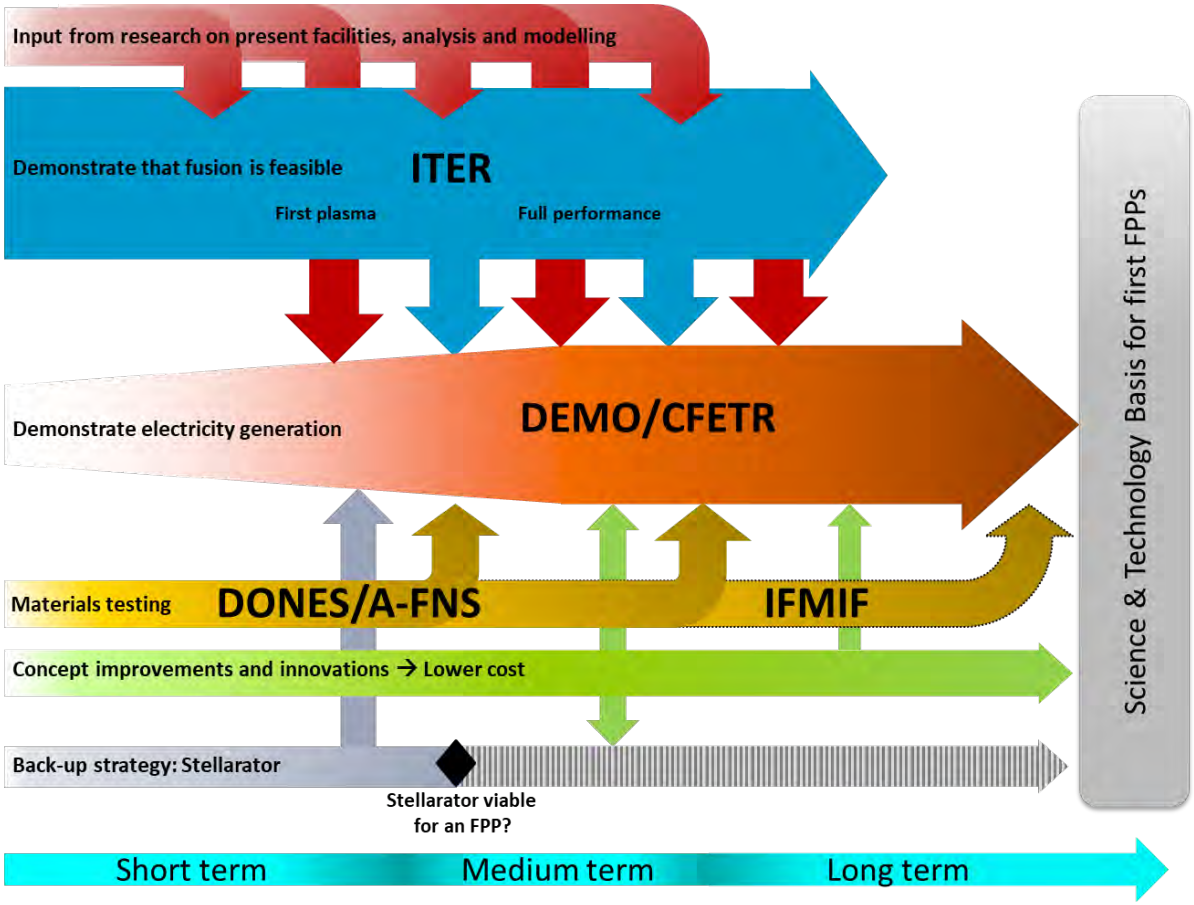

Figure 1. Schematic view of the main elements of a fusion roadmap that is common to several countries. The stellarator line is mainly in the European and Japanese roadmaps.

A second important facility included in basically all roadmaps is the demonstration reactor that will for the first time deliver electricity to the grid. In Europe and Japan this device is named DEMO (Federici et al., 2018; Tobita et al., 2019), in Korea K-DEMO (Kim et al., 2015), and in China it is known as the China Fusion Experimental Test Reactor (CFETR; Zhuang et al., 2019). These devices are all based on relatively conservative extrapolations from ITER following the rationale that obtaining a nuclear license for a new device is facilitated by exploiting technologies and components that have already been demonstrated elsewhere. Reactors following DEMO and CFETR are foreseen as first-of-a-kind fusion power plants (FPPs).

Some countries, however, prefer to pursue smaller, more flexible, facilities based on spherical tokamaks to follow ITER (Menard et al., 2016), such as the Fusion Nuclear Science Facility (FNSF; Kessel et al., 2018) in the USA and the Spherical Tokamak for Energy Production (STEP; Wilson, 2020) in the UK. Most likely these facilities must be followed by a real demonstration plant, before fusion can be commercialized. Several privately funded enterprises (Sykes et al., 2017; Sorbom et al., 2015) are also following this approach, with the special feature that high-temperature superconducting magnets are proposed to make it possible to build rather small fusion reactors, featuring a high power density. In a certain sense one could say that these approaches are depicted by the green line in Figure 1.

Since the neutron fluence in the devices following ITER (eg DEMO and CFETR) will be much higher than those in ITER, new materials need to be developed and validated. At present, this is largely pursued in Materials Test Reactors (basically fission reactors), but for testing the plasma facing components an intense neutron source with a dedicated fusion neutron spectrum is needed. The International Fusion Materials Irradiation Facility (IFMIF) is such a facility, and prototype components are presently being tested in a collaboration between Europe and Japan (Knaster et al., 2017). To accelerate the path to the realization of such a neutron source, Europe and Japan are now each proposing smaller neutron sources, IFMIF/DONES in Europe (Ibarra et al., 2018), and the Advanced Fusion Neutron Source in Japan (Ochiai et al., 2020). Spherical tokamak based devices have also been proposed as volumetric neutron sources, denoted 'Component Test Facility'.

As indicated by the red arrows in Figure 1, many operational facilities within the international fusion research program are providing input to ITER and to DEMO. Tokamaks predominate, but devices such as stellarators also give important input to the main fusion roadmap. All devices limit operation to hydrogen and deuterium plasmas to minimize nuclear activation, facilitating upgrades and the continuous evolution of experimental capabilities. The Joint European Torus (Joffrin et al., 2019), nevertheless, retains a capability for experiments with deuterium-tritium plasmas. As discussed later, several significant new non-nuclear facilities are currently in the development phase: JT-60SA, a Japan-EU collaboration (Barabaschi et al., 2019), the Divertor Test Tokamak (DTT) in Italy (Albanese et al., 2019), HL-2M (Song et al., 2019) in China and COMPASS-Upgrade (Panek et al., 2017) in the Czech Republic.

This Chapter is organized as follows. Section 2 briefly describes the key objectives, design features, major component systems and overall research framework of the ITER project. Section 3 summarizes the major considerations influencing the design of demonstration reactors based on conservative extrapolations from ITER (the DEMO reactors by Europe, Korea and Japan and the Chinese CFETR), discusses a range of concepts developed within the framework of the 'Fusion Nuclear Science Facility' and 'Pilot Plant' studies, the majority based on the spherical tokamak configuration and several seeking to exploit recent developments in high temperature superconductors, and finally comments on key prospects for stellarator-based DEMO reactors. Conceptual designs for facilities intended to provide a nuclear irradiation capability for fusion materials and components are described in Section 4, while several of the non-nuclear facilities under development are briefly discussed in Section 5.

2. ITER

2.1 Introduction

ITER is the next step fusion device, and at this moment the largest international scientific project world-wide (ITER, 2002; Bigot, 2019). It is a collaboration between China, the European Union (including Switzerland), India, Japan, South-Korea, the Russian Federation and the United States. The initial ITER collaboration was launched in November 1985 at the Geneva summit meeting between Secretary-General Gorbachev of the Soviet Union and President Reagan of the United States. After two decades of design studies, R&D and international negotiations, the ITER Agreement among the seven members was signed in November 2006 and the ITER Organization was officially established in October 2007 with its headquarters at the ITER construction site in St Paul-lez-Durance, southern France. The history of ITER is described in (Ikeda, 2010; Claessens, 2020).

As cited in the ITER Research Plan (ITER Organization, 2018), the ITER scientific goals, defined in terms of plasma fusion performance, are:

- *ITER should achieve extended burn in inductively driven plasmas with the ratio of fusion power to auxiliary heating power, Q, of at least 10 (Q≥10) for a range of operating scenarios and with a duration sufficient to achieve stationary conditions on the timescales characteristic of plasma processes.*
- *ITER should aim at demonstrating steady-state operation using non-inductive current drive with the ratio of fusion power to input power for current drive of at least 5.*
- *In addition, the possibility of controlled ignition should not be precluded.*

The technical goals, aiming to provide much of the technological basis for the design of future fusion power plants capable of generating electricity, are:

- *ITER should demonstrate the availability and integration of technologies essential for a fusion reactor (such as superconducting magnets and remote maintenance).*
- *ITER should test components for a future reactor (such as systems to exhaust power and particles from the plasma).*
- *ITER should test tritium breeding module concepts that would lead in a future reactor to tritium self-sufficiency, the extraction of high-grade heat and electricity production.*

Demonstration of the safety and environmental advantages of fusion energy is a further significant aspect of the ITER project mission. In this respect, it should be noted that ITER has undergone the full licensing procedure appropriate to a 'Basic Nuclear Installation' (INB) within the French nuclear regulatory system (see, e.g., Taylor et al. (2013)). The French Government granted the Decree of Authorization of a nuclear facility in November 2012 and ITER is now established as INB-174 within the French regulatory framework.

A cutaway view of the ITER tokamak is given in Figure 2 and the main parameters of the ITER-plasma are listed in Table 1. Extensive details on the ITER design and its technical systems can be found in papers published during the project's design and R&D phase, e.g. (ITER, 2002; Aymar et al., 2002; Shimomura, 2001), while more recent developments in ITER technology are discussed by Campbell et al. (2019).

Table 1: Main parameters of ITER

Parameter	**Value**
Major radius, R_0 (m)	6.2
Minor radius, a (m)	2.0
Toroidal field on axis, B_T (T)	5.3
Plasma current, I_p (MA)	15
Plasma elongation, κ	1.85
Plasma triangularity, δ	0.49
Edge safety factor, q_{95}	3.0
Neutral beam power, P_{NB} (MW)	33
Radiofrequency power, P_{RF} (MW)	40
Fusion power, P_{fusion} (MW)	500
Fusion gain, Q	10
Burn time (s)	300

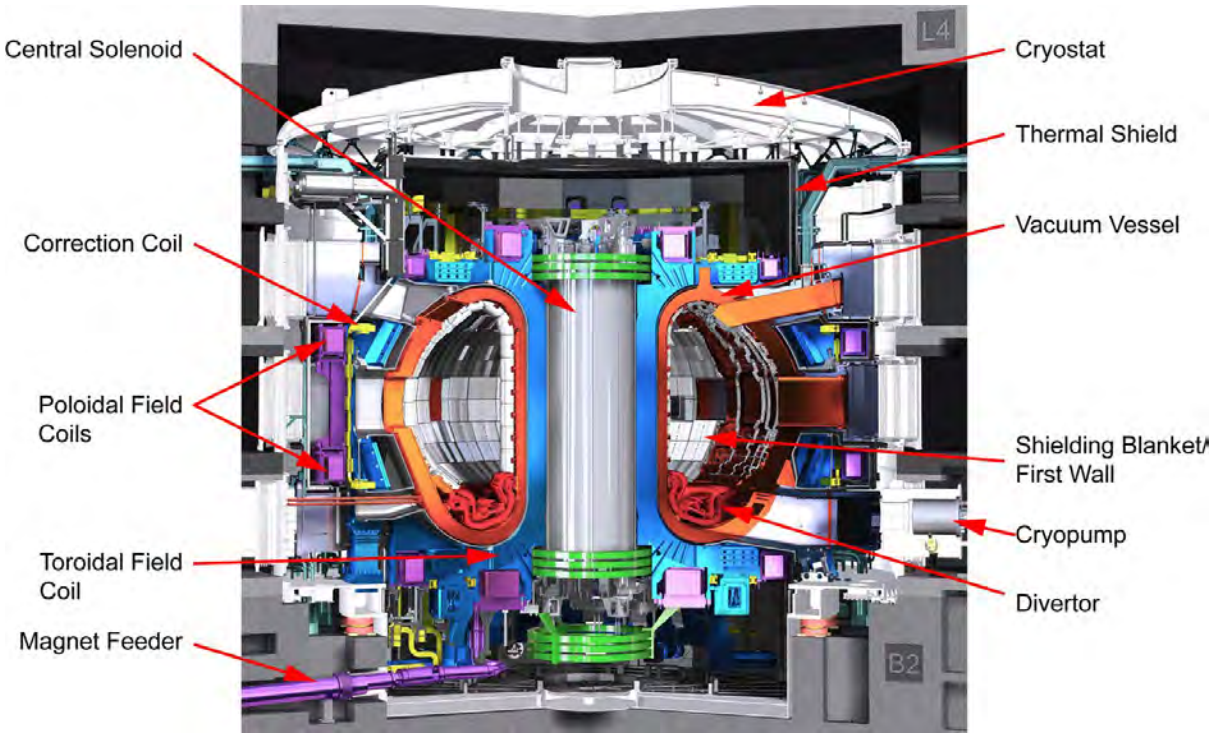

Figure 2. Schematic view of the ITER tokamak with the main components indicated (copied with permission from Campbell et al., 2019)

2.2 Tokamak core systems

As illustrated in Fig. 2, the principal tokamak core components are the vacuum vessel, plasma-facing components (divertor and shielding blanket/first wall), in-vessel control coils, superconducting coil systems (toroidal field (TF), poloidal field (PF), central solenoid (CS) and correction (CC) coils), thermal shield and cryostat.

The ITER vacuum vessel (Martinez et al., 2016), consisting of the main vessel, port structures and supporting system, provides a hermetically sealed plasma container which also fulfils the critical role of first tritium containment barrier. It is a water-cooled austenitic stainless steel (SS 316L(N)) pressure vessel with an outer diameter of 19.4 m, a height of 11.4 m and an inner volume of 1400 m^3. The main vessel is a double-walled steel structure strengthened by interspace stiffening ribs, with the space between the two 60 mm walls filled by 'in-wall' shielding in the form of modular blocks of borated and ferromagnetic steel. These blocks contribute additional neutron shielding for components external to the vacuum vessel (e.g. the superconducting magnets), while also reducing the toroidal field modulation ('ripple') caused by the finite number (18) of toroidal field coils. 44 ports in the vessel (18 upper, 17 equatorial and 9 lower ports) allow access for diagnostic systems, neutral beam injection, radio-frequency heating, fuelling and vacuum pumping, as well as providing access for remote handling systems used for maintenance and repair. The total weight of the vacuum vessel, including ports and in-wall shielding is approximately 5,200 tons.

The inner walls of the vacuum vessel, with an area of ~600 m^2, are covered by 440 actively-cooled shielding blanket modules that protect the vacuum vessel and the superconducting magnets from the heat and neutron fluxes produced by fusion reactions. Each water-cooled blanket module, fabricated from 316L(N) stainless steel, has a plasma facing surface area of ~1.5 m^2, is ~45 cm thick radially and weighs up to 4.5 tonnes. The blanket cooling water system operates at 4 MPa, with an inlet temperature of 70° C, and is capable of removing 750 MW of thermal power. A detachable first wall, fabricated from 8-10 mm thick beryllium, is mounted on the module plasma facing surface to intercept heat fluxes arriving in the form of plasma particles and electromagnetic radiation. Beryllium has been selected as the first wall material due to its low atomic number, which limits plasma contamination, and low affinity for hydrogenic isotopes, which limits fuel retention.

The divertor extracts heat, helium ash produced by the fusion reactions, unburned fuel and impurities in such a way that plasma contamination is minimized. It is formed from 54 stainless steel cassettes, each weighing ~8 tonnes, arranged to form a toroidal ring. Plasma facing surfaces ('divertor targets') are mounted on the inboard and outboard regions of the cassette designed to withstand steady state heat fluxes of 10 MWm^{-2} and slow transients of up to 20 MWm^{-2}, while the 'dome' region lying between the inner and outer targets can handle heat fluxes of up to 5 MWm^{-2}. Solid tungsten, ~8 mm thick, forms the plasma facing surfaces, due to its high melting point, low sputtering yield under plasma bombardment and low fuel retention. High pressure water cooling is used for heat exhaust, as for the shielding blanket.

The superconducting magnet systems consist of 18 TF coils and 6 CS modules wound from Nb_3Sn superconductor plus 6 PF and 18 CC coils fabricated from NbTi superconductor. All coils are cooled with supercritical helium at temperatures in the range 4.2 – 4.5 K. The D-shaped TF coils are 17 m high and 9 m wide, and each weighs ~330 tonnes. They are wound in 'double pancakes'—layers of spiraled conductor embedded in radial plates and each TF winding is encased in stainless steel. The maximum magnetic field on the coil is 11.8 T and, when fully energized, the total magnetic energy of the TF is 41 GJ. The ring-shaped PF coils, the largest having a diameter of 24 m, are mounted outside of the TF coils and operate at a maximum magnetic field of 6 T at the coil. The CS coil, with an overall height of 13 m and weighing ~1000 tonnes, consists of six independent modules, each 4 m in

diameter. With a maximum magnetic field of 13 T in the center of the coil stack and a stored magnetic energy of 6.4 GJ, the CS can sustain a 15 MA plasma current for 300 - 500 s during a high power fusion burn. The CC are much lighter, as they simply compensate for residual magnetic field errors, but the largest of these nevertheless have an area of 8×8 m^2. An overview of the ITER magnet system is provided by Mitchell and Devred (2017), while Devred et al. (2014) describe the challenges in the production of the superconductor.

The height and diameter of the ITER cryostat (Sekachev et al., 2015; Bhardwaj et al., 2016) are both ~30 m, while the structure, including the thermal shields, weighs ~4000 tonnes. With an internal volume of 16,000 m^3, this stainless steel pressure vessel provides the high vacuum (~10^{-4} Pa), cryogenic environment for the ITER tokamak core components, in particular the superconducting magnets. The cryostat has over 200 penetrations to allow for maintenance access and replacement of blanket modules and divertor cassettes, and to provide access for heating systems, diagnostics, cooling systems, and magnet feeders. It is connected to the vacuum vessel via large bellows that allow for thermal contraction and expansion during ITER operation.

2.3 Auxiliary and Plant systems

To achieve the initial conditions for achieving high fusion gain, three auxiliary heating and current drive (H&CD) systems provide a total baseline heating power of 73 MW (Singh, 2015):

- Two Neutral Beam Injectors (NBI) (Hemsworth et al., 2017) will provide a total input power of 33 MW, with provision for a third injector to allow a total beam input power of 50 MW. The injectors are based on negative ion technology (Inoue et al., 2020) operating at 1 MeV injection energy, allowing central deposition of the beam power. Near-tangential injection into the plasma allows torque input and current drive.
- The Ion Cyclotron Radiofrequency Heating (ICRF) system (Beaumont et al., 2017) injects 20 MW of power with a frequency in the range 40 – 55 MHz from two antennas located in the equatorial port plugs.
- The Electron Cyclotron Resonant Heating (ECRH) system (Darbos et al., 2016) will deliver 20 MW of power to the plasma at a frequency of 170 GHz. The gyrotron power sources are each designed to deliver 1 MW for periods of at least 1000 s. The ECRH power is injected into the plasma via launchers with steerable mirrors located in both the upper and equatorial ports of ITER.

A nominal input power level of 50 MW is foreseen for sustainment of the reference burning plasma scenario, which is predicted to generate 500 MW of DT fusion power:

ITER will have approximately 55 different diagnostic measurement systems to measure a large range of plasma and machine parameters (Donné et al., 2007; Walsh et al., 2015). The diagnostics are classified into three groups: (i) diagnostics for basic operation and machine protection, (ii) diagnostics for advanced control and (iii) diagnostics for physics evaluation and performance optimization. A large range of different diagnostic techniques is used (Inoue et al., 2020), for example, magnetic measurements, neutron emission measurements, optical systems, radiation bolometers, spectroscopy across the electromagnetic spectrum, microwave emission, transmission and reflection, and plasma-facing and operational diagnostics. For some diagnostics, the detectors must be mounted inside the vacuum vessel and great emphasis is given to ensuring their radiation hardness. Most in-vessel detectors are located deep in slots between adjacent blanket modules, to provide protection against the hostile plasma, while some diagnostics for plasma edge measurements are mounted on the divertor cassettes. Many other diagnostics have optical or microwave interfaces incorporated into dedicated vacuum vessel port plugs with complex folded optical or microwave transmission lines to reduce neutron streaming through the port plugs. Detectors and active sources, such as lasers and microwave generators, are then located in the

diagnostics building, far from the plasma. The hostile environment within the proximity of the plasma necessitates the development and application of in-situ techniques to counteract the effects of plasma bombardment of the first, plasma facing, mirrors in many optical systems, ensuring high reflectivity of the mirror surface.

A sophisticated plasma control system (PCS) combines measurements made by these diagnostic systems to sustain fusion power production via real-time control of the plasma parameters implemented via various 'actuator' systems, i.e. magnet systems, H&CD systems, fuelling and impurity injection systems (Snipes et al., 2017). At high plasma performance, the control of magnetohydrodynamic (MHD) instabilities (Lao et al., 2020) is particularly critical in ITER to maintain the fusion burn and to avoid potential damage to the first wall. For example, edge localized modes (ELMs), which expel short bursts of heat and particles, are controlled by a set of 27 in-vessel copper coils (Vostner et al., 2019). Disruptions, which produce high transient heat and electromechanical loads on in-vessel structures, must be avoided or their effects mitigated (see Lao et al., 2020; Zohm, 2020). A dedicated system, based on fragmentation of cryogenic deuterium or noble gas pellets, and referred to as Shattered Pellet Injection, SPI (Lehnen et al., 2015) will operate under PCS control to implement disruption mitigation. The PCS can also control the injection of localized H&CD to suppress MHD instabilities responsible for triggering disruptions.

Demonstration of the feasibility of producing tritium within the reactor system is a key mission of ITER, and the project will provide a unique opportunity to test prototypical in-vessel tritium breeding blankets in a real fusion environment (Giancarli et al., 2018). Several concepts for tritium breeding and high grade heat extraction will be tested in ITER using two dedicated port plugs, each allowing two distinct 'test blanket module' (TBM) designs to be exposed to the fusion neutron flux. Initially, two TBMs are planned to use water-cooling and two helium-cooling. Further details of the ITER TBM programme are discussed by Boccaccini et al. (2020).

The ITER plant systems provide key services to the tokamak and its auxiliary systems, and, in many respects, are constructed on a scale commensurate with that required in a fusion power plant. Plant systems include the Fuel Cycle (fuelling, vacuum, exhaust gas reprocessing), Remote Handling, Cryoplant, Cooling (water cooling systems, heat exchangers, waste heat exhaust), Power Supplies (steady-state and pulsed) and Waste Processing (including detritiation).

As noted above, ITER will tests concepts for tritium breeding. However, the significant amount of tritium fuel, ~14.5 kg over a period of ~20 years, required meet the project lifetime goal of achieving an average first wall neutron fluence of 0.3 MW.yr.m^{-2} means that tritium must be externally supplied from existing civil fission stockpiles and that fuel reprocessing on an unprecedented scale will be required to ensure efficient consumption of tritium. A large-scale tritium reprocessing plant therefore forms the core of the ITER Fuel Cycle system (Boccaccini et al., 2020): an annual tritium reprocessing capability corresponding to ~25 times the onsite tritium inventory will be required. A substantial high vacuum pumping capability is a further critical element. The total volume of the ITER vacuum system (Day et al., 2008) exceeds 10,000 m^3 (cryostat: 8500 m^3, vacuum vessel: 1330 m^3, neutral beam injectors: 180 m^3 each). The central part of the roughing system consists of newly developed cryogenic viscous flow compressors in combination with Roots mechanical pumps, while the facility also features a set of six cryopumps for the main vacuum vessel, four for the neutral beam system and two for the cryostat. These pumps, cooled by supercritical helium, are coated with activated charcoal as sorbent material, in particular for helium pumping. Finally, fuelling of DT plasmas by gas injection and cryogenic pellet injection closes the fuel cycle. Further considerations related to the design of reactor-scale fuel cycle systems can be found in Boccaccini et al. (2020).

ITER is equipped with one of the world's largest cryoplants (Monneret et al., 2017) - only the distributed system for the Large Hadron Collider has a greater cooling capacity. It consists of two large nitrogen refrigerators and three large helium refrigerators, which provide the necessary cooling for the superconducting magnets. It also supplies the six cryopumps that operate at a temperature of 4 K, the magnet current leads that operate at 50 K and the thermal shields within the cryostat that are cooled to 80 K. The installed cooling power is 75 kW at 4.5 K (helium) and 1300 kW at 80 K. The ITER tokamak and the auxiliary systems will produce on average 500 MW of heat during a typical plasma pulse cycle, with a peak of 1.1 GW during the plasma burn phase, and this needs to be dissipated to the environment. Heat generated by the plasma is transferred via the Tokamak Cooling Water System, TCWS (Lioce et al., 2019), to the intermediate Component Cooling Water System (CCWS; Kumar et al., 2013), which is a closed loop system that transfers the heat to the Heat Rejection System (HRS). Water from the HRS is ultimately discharged into the nearby canal after monitoring to ensure that it fulfils the stringent environmental release criteria.

Robust remote handling techniques are being developed to support in-vessel maintenance and repairs (Damiani et al., 2018; Federici et al., 2020). Special remote handling tools will be able to replace heavy components such as the blanket modules, divertor cassettes and the port plugs, with weights of up to 50 tons. A substantial Hot Cell Facility, HCF (Friconneau et al., 2017), will permit maintenance and processing of irradiated and tritiated components that have been removed from the tokamak. Transportation between the tokamak and the HCF will be carried out using a sealed transport cask. Radioactive waste will be produced during ITER operation and decommissioning (Rosanvallon et al., 2016) due to the replacement of components, as well as from process and housekeeping waste. The waste consists of components activated by neutrons with energies of up to 14 MeV, and contaminated by activated corrosion products, activated dust (including beryllium and tungsten dust) and tritium. To satisfy French regulatory requirements, facilities are included in the ITER Hot Cell complex for the treatment and interim storage of the waste. This complex, equipped with an extensive remote handling capability, will provide a secure environment for the processing, repair or refurbishment, testing, detritiation and disposal of activated ITER components.

2.4 ITER Research Plan

The ITER Baseline Schedule foresees a phased transition from facility construction to plasma operation (the 'Staged Approach'), with the scope of the associated research program, as defined by the ITER Research Plan (IRP) (ITER, 2018), expanding as the facility capabilities are increased over a period of approximately 10 years (figure 3). Within the IRP, these first 10 years of ITER operation are sub-divided into three phases: First Plasma (FP), Pre-Fusion Power Operation (PFPO, subdivided into two stages) and Fusion Power Operation (FPO). During the FP and PFPO phases ITER will operate only with hydrogen and helium plasmas, while the FPO phase will focus on optimization of fusion power production in DT plasmas.

During the First Plasma phase, scheduled for late 2025 and targeting plasma currents in the range 100 – 500 kA, the magnets, the vacuum vessel and the cryostat will be qualified and the most basic auxiliary systems commissioned. These commissioning and experimental activities terminate in an Engineering Commissioning phase to commission the superconducting magnet systems to full current. The PFPO-I and PFPO-II programs are dedicated to a phased commissioning of key hardware systems associated with a gradual increase in plasma parameters and in the sophistication of plasma operating scenarios. Thus, the blanket modules/ first wall, divertor, full ECRH system and a range of diagnostic and dedicated control systems will be installed in advance of PFPO-I, allowing routine operation at plasma currents of up to 7.5 MA and toroidal fields in the range 1.8 – 5.3 T with heating powers of up to 20 MW. A range of plasma operating regimes and plasma control schemes, including disruption avoidance and mitigation, will be commissioned and explored during this program. The

full H&CD capability and an extended set of diagnostic systems will be added in advance of PFPO-II. This will support operation at full technical performance (15 MA/5.3 T) with up to 73 MW of heating power and the implementation of an extensive program of plasma and plasma control scheme development, with plasma pulse durations of at least 100 s, in preparation for the transition to DT plasma operation.

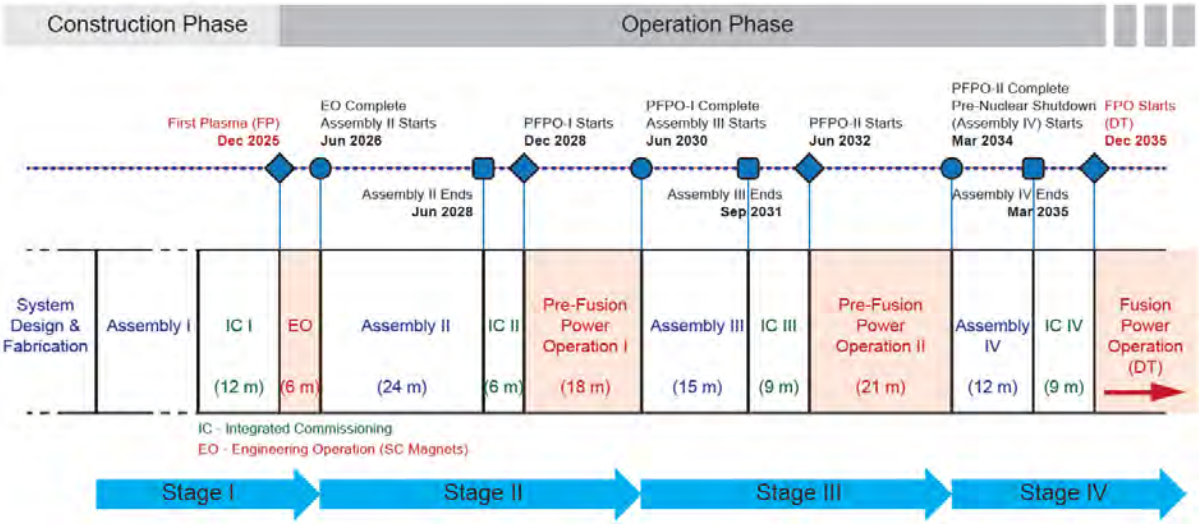

Figure 3. Schematic time sequence of the first 10 years of ITER operation in the Staged Approach (adapted with permission from Fig. 5 of Campbell et al., 2019).

Long-range plans foresee final preparations for DT operation being made in 2034-2035, including the final commissioning of the DT fuel cycle and the installation of additional DT-relevant diagnostics. Following authorization by the nuclear authorities, deuterium plasma operation would be launched in early 2035, followed by the transition to full DT operation in the course of 2035. Operating on a two-year cycle of 16 months plasma operation and 8 months maintenance, a series of experimental campaigns would explore optimization of fusion power production in a range of 'baseline' plasma scenarios, as detailed in Table 2. Initially, the program is planned to address the achievement of a fusion gain, Q, of at least 10 at fusion powers of up to 500 MW using nominal plasma parameters of 15 MA/5.3 T, and with the burning plasma duration being extended towards the range 300 – 500 s as operational experience accumulates. Alternative scenarios which current experiments indicate as particularly promising include the 'hybrid' scenario, operating in the range 12 – 14 MA with a significant component of non-inductive current drive. A further key aim of the DT experiments is the achievement of fully non-inductive steady-state plasma operation at lower plasma currents, ~9 MA, with $Q \geq 5$ and pulse durations of up to 3000 s.

Table 2: Main parameters of the ITER baseline reference scenarios (Campbell et al., 2019)

Parameter	**Inductive**	**Hybrid**	**Non-inductive**
Plasma current, I_p (MA)	15	13.8	9
Energy confinement time, τ_E (s)	3.4	2.7	3.1
Confinement enhancement $H_{H98}(y,2)$	1.0	1.0	1.6
Pressure figure of merit, β_N	2.0	1.9	3.0
Average electron density $\langle n_e \rangle$ (10^{19} m^{-3})	11.3	9.3	6.7
Fusion power, P_{fusion} (MW)	500	400	360
Fusion gain, Q	10	5.4	6
Burn time (s)	300-500	>1000	~3000

While the fully non-inductive steady-state scenario (i.e. with zero flux swing in the CS) is anticipated to provide the operational basis for future fusion reactors, ITER can also explore alternative operating scenarios to those listed in Table 2, whether developed in ongoing experiments in smaller devices, or in ITER's experimental program. The DT operations phase will, in addition, incorporate significant fusion technology studies in support of DEMO and future reactors, the most significant being the demonstration of tritium breeding and high grade heat extraction from the TBMs which will be exposed to the DT neutron flux.

3. Demonstration reactors

3.1 Background

With the ITER project well under way, the nations engaged in magnetic fusion R&D are now determining the necessary science and technology developments required to harness fusion energy. This includes, primarily, progression towards a device capable of demonstrating the production of few hundred MW of net electricity, feasibility of operation with a closed-tritium fuel cycle, maintenance systems capable of achieving adequate plant availability, a high level of safety and low environmental impact. This is known as a DEMOnstration Fusion Power Plant (DEMO).

Europe and Japan envision that ITER should be succeeded by the construction and exploitation of DEMO, the final step before the first commercial power plant. A dedicated divertor test tokamak (DTT), to investigate the problem of power exhaust and demonstrate performance of advance divertor solutions, and a neutron-irradiation facility to qualify materials (IFMIF–DONES) are included in this strategy. Stellarators are also being pursued, the largest devices being LHD (Japan) and Wendelstein 7-X (Europe). China has an ambitious plan to exploit fusion energy for electricity production as quickly as possible to offset the foreseeable large increase in energy demand. The "Chinese Fusion Engineering Test Reactor (CFETR)" facility is currently in the conceptual design development phase with construction planned by the end of the 2020s. South Korea has begun pre-conceptual design work on a DEMO device to develop technology solutions, denoted 'K-DEMO-1', with the intention of starting construction in the late-2020s and beginning operation in 2040. After a reconfiguration of the internal components, the second phase ('K-DEMO-2') will be launched, leading to a full demonstration of industrial scale electricity generation from a fusion plant. Other communities, e.g. the US and India, view DEMO as the last step before commercialization, but both consider that an intermediate step between ITER and DEMO is required. There is considerable deliberation over the scope of such a device and delay in exploiting fusion energy implied by an additional intermediate step is an issue. Finally, the Russian Federation is considering both 'pure' fusion machines and fission–fusion hybrids in their strategy.

The construction, commissioning and operation of ITER are central elements in all fusion development roadmaps. However, while the contribution of ITER to fusion technology is undeniable, large gaps towards DEMO remain and there is an urgent need for continued and vigorous R&D in areas such as fusion grade materials, tritium breeding, plasma exhaust solutions, heating and current drive systems (especially in terms of efficiency), and remote handling. The integration of these technologies to build a reliable device is recognized as being, probably, the greatest challenge ahead. ITER design and construction activities have, nevertheless, yielded several important lessons for those responsible for DEMO design:

(1) the importance of thermal transients for in-vessel component design;
(2) strengthening of nuclear design integration and nuclear safety culture during all design phases;
(3) implications of design changes imposed on ITER by regulatory bodies, derived from increasingly stringent nuclear safety regulations;
(4) the criticality of a robust maintenance plan with clear provisions to access areas where contamination and activation could be higher than initially considered;
(5) the need to address more systematically plant layout considerations, including cooling loops and auxiliary systems, and to provide adequate space to integrate all equipment, particularly in the tokamak building.

3.2 Demonstration reactors based on extrapolations from ITER

Defining appropriate plant design parameters and technical features starts with the definition of the plant requirements and involves trade-offs between the attractiveness and technical risk associated with the design options. Some of the physics assumptions (e.g. energy confinement, plasma pressure, H-mode access threshold, bootstrap current fraction, etc.), and technology assumptions (e.g. allowable divertor heat loads, structural material neutron-load limits, maximum field in the superconducting magnets, plant thermodynamic efficiency, wall-plug efficiency of Heating and Current Drive systems, etc.) play a major role in the tokamak dimensioning process. Schematic drawings of the current designs of the EU DEMO and CFETR are shown in Fig. 4 and 5, respectively. The considered design parameters of these devices, along with those of JA-DEMO and K-DEMO are shown in Table 3.

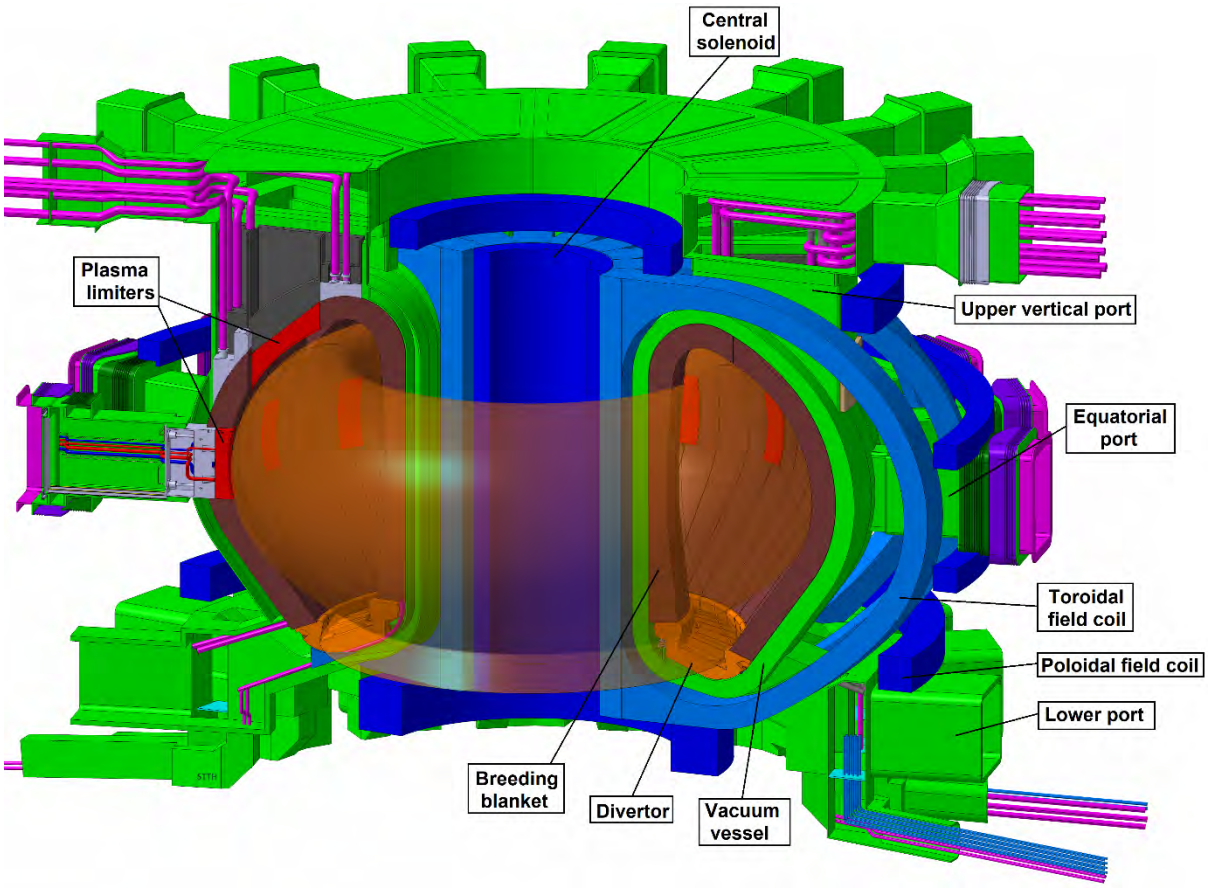

Figure 4. Schematic drawing of EU DEMO with the various component indicated. © EUROfusion

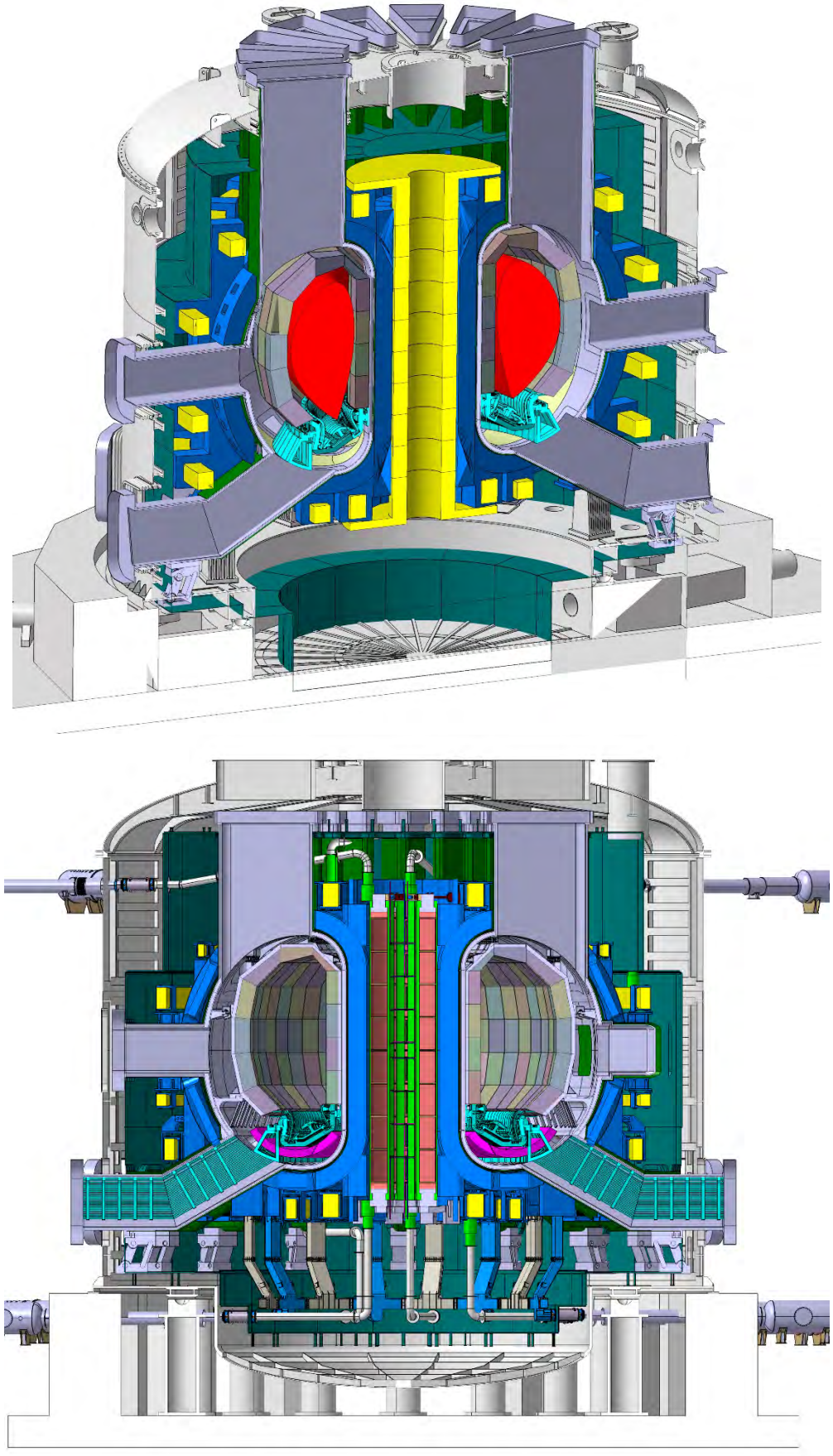

Figure 5. Schematic drawing of CFETR (courtesy ASIPP, China).

Table 3. Main machine parameters for future devices in EU, Japan, China and South Korea DEMOs. Data of JA DEMO largely extracted from Tobita et al., 2019; data of CFETR largely extracted from Zhuang et al., 2019; data of K-DEMO extracted from Kim et al., 2015; Neilson et al., 2014 and Kang et al., 2017.

Parameters	**Symbol**	**EU DEMO (Pulsed/ 2hrs)**	**JA DEMO (Steady-state)**	**CFETR (Steady-state)**	**K-DEMO (Steady-state)***
Major, minor radius	R_p, a (m)	9.0, 2.9	8.5, 2.42	7.2, 2.2	6.8, 2.1
Aspect ratio	A	3.1	3.5	3.3	3.2
Magnetic field on axis	B_T (T)	5.9	5.9	6.5	7.4
Plasma current, edge safety factor	I_p (MA), q_{95}	18, 3.9	12.3, 4.1	12-14/5	>12, <8.0
Elongation, triangularity	κ_{95}, δ_{95}	1.65, 0.33	1.65, 0.33	2, 0.4-0.6	2.0, 0.63
Fusion and auxiliary power	P_{fus} (GW), P_{aux}(MW)	2.0, 50	1.5, 83.4	0.1-2.0/80	2.2-3.0, 80-130
Net electrical power	$P_{el,net}$ (GW)	0.5	>0.25	0-0.8	0.4-0.7
Confinement factor	HH_{98y2}	~1	1.3	0.7-1.6	1.6
Normalized beta	β_N	2.6	3.4	1-3	<4
Bootstrap fraction	f_{BS}	0.39	0.61	0.4-0.6	>0.6
Relative density to Greenwald density	n_e/n_{GW}	1.2	1.2	0.5-1.3	1.25
Average power load on structure	A_{NW} (MW/m^2)	~1	~1	0.1-2.5	1.6-2.0
Structural material		EUROFER for the blanket and AISI 316 for the vacuum vessel	FH82 for the blanket and AISI 316 for the vacuum vessel.	ODS Ferritic Martensitic steel for the blanket	Reduced-Activation Ferritic Martensitic steel for the blanket
Divertor		Single-null water-cooled; W-armor.	Single-null water-cooled; W-armor.	Advanced divertor	Double-null water-cooled W-armor
Breeding blanket (TBM)		WCLL/HCPB	WCPB	WCLL/HCPB	HCSB/WCCB
Toroidal field coils		LTSC magnets Nb_3Sn (grading)	LTSC magnets Nb_3Sn	NbTi/ITER Nb_3SN/ high Nb_3SN	LTSC magnets Nb_3Sn
Lifetime 1st/2nd blanket	(dpa)	20/50	20/TBD	10/20	TBD
Remote maintenance		blanket vertical RH / divertor cassettes	blanket vertical RH / divertor cassettes	blanket vertical RH / divertor cassettes	blanket & divertor cassettes vertical RH
Balance-of-Plant		yes	yes	yes	yes

* Results of an optional study

A major difference between the EU DEMO and CFETR (Zhuang et al., 2019) design concepts is that the CFETR design assumes steady-state operation, with a significant current-drive fraction, and hence low-density operation (which is a challenge for the divertor). The EU DEMO design is based on

operation in 2-hour pulses and relies on a conventional, ideally ELM-free, H-mode scenario with an emphasis on power exhaust issues. This is not yet a fixed design choice, but rather a "proxy" to be used to identify and resolve crucial design integration problems (Federici et al., 2016; Federici et al., 2018). Considerations are also given to a design capable of a short pulse mode operation (e.g., 1 hour) for nominal extrapolated performance (H_{98}=1.0) and capable of moving to steady-state operation, while maintaining the same fusion power and net electrical production, when it proves possible to access plasma conditions with better confinement. However, this option requires greater confidence in physics extrapolation and highly reliable and efficient current-drive and control systems, which will require further development. In contrast, a key design consideration for CFETR is the reliance on 'staged operation' spanning a wide operating range (see Table 3), for the progressive development of the plasma physics, materials science and technology over the operational lifetime of the plant to achieve performance improvements through system and/or component upgrades.

Although many discussions are ongoing regarding the possibility to achieve fusion power from smaller and cheaper devices to be built on a fast timescale, there is no magic bullet to solve the integrated design problems: squeezing one element of the design inevitably exacerbates design challenges elsewhere. The design of EU DEMO is based on the present physics knowledge – i.e. the H-mode scaling, exhaust and technology – and on the experience gained in the design and construction of ITER. It is not based on an a priori decision to design a large-scale device (Federici et al., 2016).

It is essential to address integration issues in the design activity as early as possible to avoid the development of design solutions that cannot be integrated in practice. In addition, fusion is a nuclear technology and will be assessed with full scrutiny by nuclear regulators. In this context, shielding, remote handling, safety, and licensing considerations all play significant roles in the design.

System codes (see Kovari et al., 2014; Kovari et al., 2016; Reux et al., 2018) for the full DEMO power plant are being used in Europe to underpin DEMO design studies and find meaningful design points (Kemp et al., 2018). These codes are used to find solutions with a minimum major radius, which is a rough proxy for the cost of the device. Determining the available design space for DEMO has been the subject of recent European studies (Federici et al., 2016; Federici et al., 2019; Federici et al., 2017; Siccinio et al., 2019). Three overarching limitations preventing further reductions in major radius are: (1) the divertor power handling, (2) the maximum field in the conductor of the toroidal field (TF) coils and the stress in the coil casing, and (3) the access to the H-mode:

(1) The minimum size of DEMO is currently limited by divertor exhaust power handling for a given machine size, represented in systems code terms as $P_{sep}\,B/qAR_0$, where P_{sep} is the power crossing the separatrix, B is the toroidal field in the plasma, q is the safety factor at the plasma edge, A is the aspect ratio, and R_0 is the machine major radius (Federici et al., 2019).

(2) The magnet performance is a further limit on DEMO sizing: the achievable field is limited by the stresses in the mechanical structures of the coils, rather than the superconductor performance. Forces vary with B^2, and since the coil cannot expand toroidally, it must become radially larger, rapidly limiting how small the machine can become. With an aspect ratio of 3.1, space for a breeding blanket, and stress limits of <700MPa in the structural coil materials, targeting a field of 5T in the plasma leads to a device with R_0>7m without considering other limitations. A growth in the coil allows higher fields representative of high-temperature superconductors (HTS), but without a corresponding increase in the stress limit, results in a larger machine (albeit, one with improved plasma confinement). To an

extent, this can be overcome by excluding tritium breeding from the inboard side to reduce the plasma-magnet distance, but this seriously compromises the ability to breed fuel.

(3) In order to access H-mode, it is assumed that the amount of power crossing a flux surface just inside the separatrix must exceed the L-H transition threshold power P_{LH}. At present, it is assumed that $P_{sep} > P_{LH}$ for DEMO, as it is likely that P_{sep} will need to be higher than P_{LH} in order to achieve sufficient controllability and confinement quality. Using the Martin scaling (Martin, 2008) for P_{LH} and the Greenwald scaling (Greenwald, 1988) for the density limit, it can be found that for a fixed P_{sep}/R_0 (i.e. divertor protection figure of merit) increasing the ratio of P_{sep}/P_{LH} can only be satisfied by reducing the magnetic field (Wenninger et al., 2015).

Allowing a variation in aspect ratio, R/a, appears to overcome some of these limits. As aspect ratio falls, elongation can be increased and a higher β_N is achievable; however the increased minor radius means that the field in the plasma is lower and the actual plasma pressure does not change much. For a given achievable field at the TF coil, there is no significant change in power density, although lower aspect ratio designs can deliver higher absolute power due to increased plasma volume (but must still respect power exhaust constraints). This increased power comes at the cost of TF coils that have a larger cross-sectional area, to accommodate the increased plasma volume.

Taking all these elements into account using more detailed models, and allowing for some conservatism, a device of R_0~9.0m is required. To significantly reduce the size requires advances in plasma physics (higher energy confinement, control and diagnostics in a fusion environment, plasma scenarios that reduce the power density to the divertor target, and highly reliable techniques to mitigate the transient effects of ELMs or exploitation of ELM-free scenarios); materials and design solutions to handle higher power densities in multiple parts of the reactor during steady-state operation and transients; remote handling maintaining high availability with restricted access; and improved magnets capable of higher fields and handling the resulting structural stresses. This must be achieved while integrating nuclear safety in the design *ab initio*, and without jeopardizing reliability. This does not mean that the EU-DEMO is low-risk, but that the approach chosen is to minimize the risk in extrapolation.

An increased appetite for risk on fusion performance would lead to design changes, which may ultimately reduce the size of DEMO. The first is a reduction in conservatism – a more complete scientific and technical basis allows a reduction in performance margins on extrapolation and increased confidence in plasma control at high radiative fraction, plasma-facing component (PFC) surface erosion rates, or higher β_N. This may be offset by the need to operate in e.g. ELM-free regimes. It is anticipated that the ITER and DEMO research programs will improve understanding and reduce uncertainties before the DEMO design point is finalized. If the high-level goals of DEMO are relaxed (e.g., through a reduction in target electricity production or tritium self-sufficiency, or less targeted technology transfer to a fusion power plant), size savings can be achieved. Pulse length could also be shortened (to save solenoid space) or lower aspect ratio explored (this can generally achieve higher bootstrap current fraction, supporting longer pulse length without additional auxiliary current drive). In the first case, the DEMO mission is compromised and in the second, the design is based on a reduced scientific basis.

3.3 Fusion Nuclear Science Facilities and Pilot Plants

Studies have been performed to evaluate what additional science and technology advances would be required to significantly reduce the scale of the devices summarized in Table 3 and/or to pursue a complementary mission to those of ITER and DEMO to make unique contributions to the world

fusion development program. The Fusion Nuclear Science Facility (FNSF) (Peng et al., 2009; Menard et al., 2016; Kessel et al., 2018) aims to create a fusion-nuclear environment representative of fusion power plants to establish a materials and component operational database before proceeding to larger electricity producing devices (see Fig. 6). To be relevant to future fusion power plants, an FNSF facility and program must also utilize and advance fusion-relevant materials for radiation resistance, low activation, operating temperature range, chemical compatibility, and plasma-material interaction damage resistance.

In an FNSF program, blanket material and component development and testing leading to tritium self-sufficiency and high thermal conversion efficiency are high priority mission elements. For FNSF concepts pursued in the U.S., full poloidal Dual Coolant Lead Lithium (DCLL) blankets are pursued as the baseline blanket concept due to the potential for high operating temperature and thermal conversion efficiency. Helium Cooled Lead Lithium (HCLL) and Helium Cooled Ceramic Breeder/Pebble Bed (HCCB/PB) are considered alternate blankets to be developed in FNSF if necessary to mitigate DCLL risks in liquid metal breeder technology and the flow channel insert development (Kessel et al., 2018). Detailed 3D neutronics and tritium breeding ratio calculations are critical to assess the effects of test blanket modules and non-breeding regions (e.g. materials test modules, ports for heating and current drive systems, diagnostics, and disruption mitigation) on the viability of T self-sufficiency in FNSF.

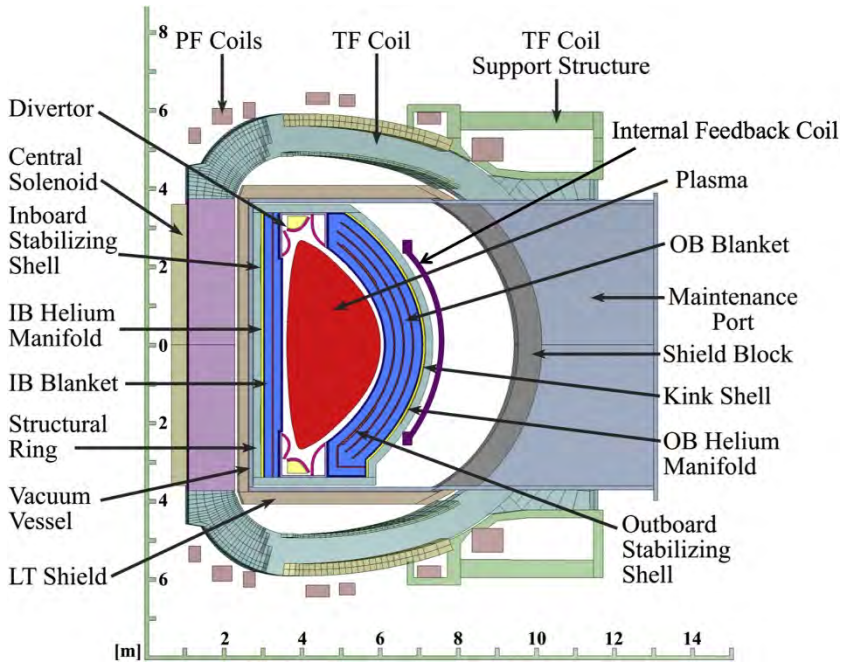

Figure 6. Cross section of the Fusion Nuclear Science Facility (reproduced with permission from Kessel et al., 2018)

A conventional aspect ratio (A=4) and steady-state FNSF operating range has been identified (Kessel et al., 2018), and detailed analysis has been carried out for an operating point with R = 4.8 m, a = 1.2 m, I_P = 7.9 MA, B_T = 7.5 T, $\beta_N < 2.7$, $n/n_{Gr} = 0.9$, $f_{BS} = 0.52$, $q_{95} = 6.0$, $H_{98} \sim 1.0$, and Q = 4.0. This operating space is found to be robust to parameter variations and operates ~35% below the divertor exhaust power parameter limit of P_{sep} B / q A R_0 = 9.3MW/m used for EU DEMO (Federici et al., 2019). At full performance the A=4 FNSF generates 1.2MW/m^2 average neutron wall loading, which is comparable to the EU DEMO1 value, but with a major radius approximately half that of DEMO1 (4.8m vs. 9.1m) and with one quarter of the fusion power (0.52GW vs. 2.04GW). The FNSF facility discussed here (with A=4) was not designed to generate net electricity but has an equivalent

engineering gain near 1 (Q_{eng} = 0.86) and could access Q_{eng} > 1 (equivalent) with increased confinement enhancement factor, i.e. H_{98} > 1.0. It also aims to access higher shaping (higher elongation and triangularity) and exploits a double-null divertor configuration to increase stability limits. The design uses a radial port maintenance scheme, which differs from the vertical port maintenance approach used by EU DEMO, CFETR, and several other DEMO concepts. The device maintainability and availability dependence on maintenance approach is an active area of research.

Lower aspect ratio and smaller major radius FNSF concepts based on the spherical tokamak (ST) have also been explored. An ST with copper toroidal field coils is a promising candidate for the FNSF application due to its potentially high neutron wall loading and modular configuration (Menard et al., 2016), with fusion-relevant neutron wall loadings of ~1 MW/m^2 possible in devices as small as R=1m, at fusion powers of 50-100MW, and a vertical maintenance scheme enabling removal of all in-vessel fusion core elements. An ST-based FNSF with R=1m cannot achieve a Tritium Breeding Ratio (TBR) ≥ 1 (TBR without Be enrichment = 0.85-0.9) and would require T from external sources. Larger ST devices with R ≥ 1.7m and P_{fus} = 150-200MW are projected to achieve TBR ≥ 1. Potential disadvantages of the ST-based FSNF device include the lack of a central solenoid for current initiation or sustainment, neutron embrittlement of the central Cu TF magnet, hundreds of MW of resistive power dissipation in the TF magnet, and a less developed physics basis for energy confinement and non-inductive current sustainment. The NSTX Upgrade (Menard et al., 2012) and MAST Upgrade (Chapman et al., 2015) facilities and research programs are strongly aligned with addressing these ST physics issues, with NSTX-U emphasizing core transport and stability and non-inductive sustainment, and MAST-U emphasizing power exhaust mitigation using novel long-legged divertor capabilities and core-edge integration with such divertors.

While the FNSF approach emphasizes nuclear component and blanket development to demonstrate tritium self-sufficiency and steady-state plasma operation, a further related mission is that of achieving electricity break-even (Q_{eng} ≥ 1) in a so-called “Pilot Plant” (Dean et al., 1991; Dean et al., 1992; Menard et al., 2011). Such a mission places lower priority on very high neutron fluence operation. For advanced tokamak (AT)-based Pilot Plant operation, both higher maximum field and higher effective current density within the inboard leg of the toroidal field coil was found to be a key enabling capability for achieving electricity break-even in a smaller-major-radius R=4m, A=4 tokamak (Menard et al., 2011). Toroidal field magnets using REBCO HTS tapes with very high peak on-coil magnetic field, B_{max} = 23 T, have been proposed to access very high toroidal magnetic field B_0 = 9.2 T at the plasma geometric center in an R=3.3m compact pilot plant, “ARC”, producing 190MW of net electric power (Sorbom et al., 2015). Compact pilot plant concepts, such as ARC (see Fig. 7) motivate the development of several potential innovations including high-field-side lower-hybrid current drive for steady-state operation, demountable superconducting TF magnets for fusion core access and maintenance, an immersion blanket using the molten-salt FLiBe as a single-phase, low-pressure, single-fluid coolant, and a long-legged tightly-baffled divertor power exhaust scheme (Wigram et al., 2019) compatible with the immersion blankets and elevated core confinement (H_{98} = 1.8).

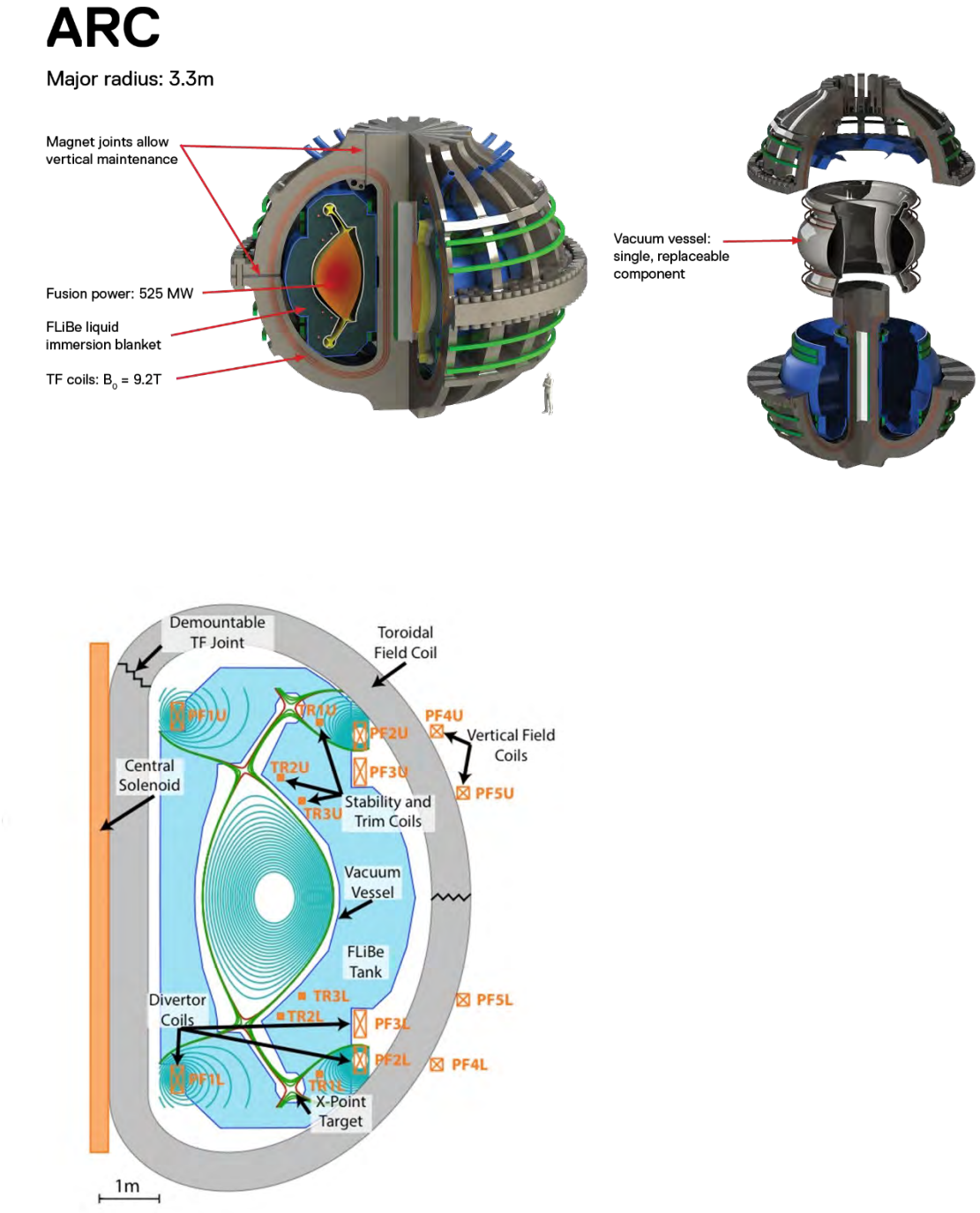

Figure 7: (a) Rendering of the ARC power plant (adapted from Sorbom et al., 2015; Figure credit: MIT PSFC); and (b) schematic diagram of the long-legged X-point divertor (reproduced with permission from Kuang et al., 2018).

Lower aspect ratio fully-non-inductive tokamak pilot plant concepts with A=2, R=3.0m, B_T = 4T, P_{fus} = 500-550MW, Q=10, and P_{net} = 50-100MW which exploit the projected very high current density of REBCO-based HTS superconducting TF magnets have also been developed (Menard et al., 2016). A proposed A=2 HTS pilot plant uses full poloidal DCLL blankets, as proposed for the A=4 FNSF, but has a vertical maintenance scheme similar to the EU DEMO approach. Neutronics calculations for the A=2 HTS pilot plant indicate that an inboard water-cooled shield combined with a thin inboard DCLL breeding region (and a thick outboard breeding blanket) can achieve TBR > 1, high neutron flux and

fluence, and tritium and electrical self-sufficiency. Such a device may reduce the magnet mass per unit fusion power relative to higher aspect ratio configurations and may offer core stability and confinement advantages (Menard, 2019). However, at these low aspect ratios there is only room for a small central solenoid, so non-inductive current formation and/or overdrive would be needed to access the full flat-top operating current of 12-13MA. Furthermore, as is the case for the ST-based FNSF, the physics basis for higher-field low-A tokamaks with A=1.7 to 2.2 has not yet been established and will need to be supported by research on NSTX-U, MAST-U, and ST-40 (Windridge, 2019).

A key question to be addressed in choosing the optimal aspect ratio for fully-non-inductive pilot plants is how energy confinement scales versus aspect ratio between spherical and more conventional tokamak aspect ratios, i.e. covering the range A=1.7 to 2.4 (Menard, 2019). If high confinement and high-bootstrap fraction scenarios can be realized in near-term STs and if high-field high-current-density TF magnets can be realized (Windridge, 2019; Sorbom et al., 2015), a more modular path to fusion energy development may become feasible (Chuyanov and Gryaznevich, 2017). The UK government has also expressed interest in advancing the ST for fusion energy through the Spherical Tokamak for Energy Production (STEP) programme (Wilson, 2020). STEP is proposed as a staged programme to design and build the world's first compact fusion reactor based on the ST by 2040.

3.4 Prospects for Stellarator-based demonstration reactors

The stellarator (Yamada, 2020) is a promising alternative to the tokamak, offering inherently steady-state operation and enhanced plasma operational reliability without severe disruptions. It is therefore being pursued internationally as a potential fusion power plant candidate. The freedom to shape a stellarator plasma in three dimensions opens up a path to resolve plasma and engineering issues by computational design rather than by relying on specific plasma regimes. Specifically, stellarators possess 40-50 degrees of freedom in shaping the magnetic field, providing a virtually infinite configuration space. However, while significant progress has been made in the physics optimisation, the challenges in the area of stellarator engineering remain to be addressed. A variety of stellarator concepts exist, the most studied concepts being heliotrons and advanced stellarators (including compact designs) (MFE16, 2016).

As for tokamaks, some of the greatest challenges are in engineering and technology (e.g. 3D non-planar magnet design, heterogeneous neutron loads, divertor heat loads, 3D blanket design and segmentation, remote maintenance, etc.). Detailed studies of these issues are limited, but these aspects have gained more interest in recent years and it is expected that, with the success of devices such as W7-X and LHD, further attention will be drawn to stellarator-specific reactor-relevant engineering and technology aspects. Similar to the physics optimisation, stellarator engineering offers tremendous potential to address challenges by computational design and optimisation.

Design studies for a stellarator-based DEMO device are less advanced than those for tokamak-based devices, though conceptual studies of fusion reactors based on extrapolations of the most favoured stellarator configurations have been developed (see figure 8), e.g. HELIAS 5-B (Schauer et al., 2011, 2013), extrapolated from the W7-X design (Grieger and Milch, 1993; Grieger et al., 1992), and FFHR (Sagara et al., 2012) a refinement of the heliotron concept, where extensive experimental experience has been accumulated, including more than two decades of operation of the Large Helical Device, LHD (Iiyoshi et al., 1999).

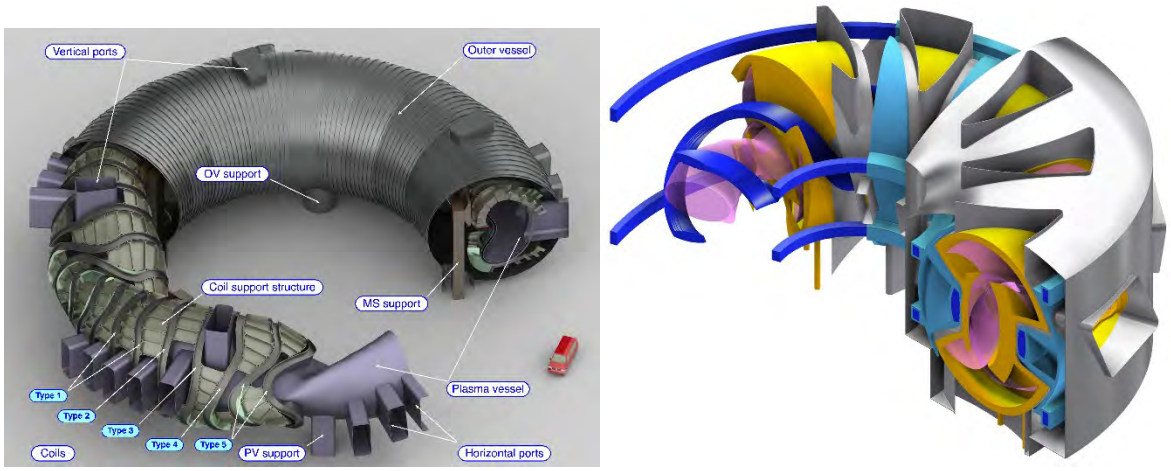

Figure 8: HELIAS 5-B, design study for an advanced stellarator fusion power plant (left; reproduced with permission from Schauer et al., 2013) and FFHR-d1, a heliotron type design based on LHD (right; reproduced with permission from Tamura et al., 2015).

With a major radius, R=22 m, HELIAS-5B has a slightly larger aspect ratio, R/a = 12, than that of W7-X to accommodate space for the blanket. The space between the plasma and the magnetic field coils is a limiting factor in stellarator designs and space requirements for a blanket impose a lower limit on the device size. The space between the coils is also an important factor for port-based maintenance, limiting the maximum size of the blanket segments. Therefore, optimised coil designs are under investigation that offer a higher accessibility without compromising the magnetic configuration (Gates et al., 2017). Using Nb_3Sn superconductor technology similar to ITER, which allows a field of 5 - 6 T on-axis, the 50 non-planar field coils are roughly the same size as the ITER toroidal field coils, allowing off-site fabrication. High-temperature-superconductors are also under consideration, but the associated quench protection and electromagnetic forces are challenging aspects that need detailed investigations.

Winding of the large helical coils, which must be prepared on-site, is a particular challenge for the FFHR design. The large poloidal field coils also require on-site assembly. Joint-winding of large-current capacity conductors employing high-temperature superconducting tapes that could be connected on site by mechanical connection offers a potential alternative. Sufficiently low joint resistance has been confirmed by a prototype conductor (Yanagi et al., 2015) and a large-scale fabrication method is under investigation. On the other hand, this concept incorporates large gaps between the helical windings, which serve as access points for port-based remote maintenance.

To provide tritium breeding in HELIAS-5B, adaptation of tokamak DEMO blanket concepts is under study. The HCPB concept (Boccaccini et al., 2020) appears favourable due to its low space requirements and very high tritium breeding ratio (TBR = 1.38 for HELIAS 5-B (Häussler et al., 2018)).The FFHR blanket design uses a molten salt (LiF-BeF2) self-cooled liquid tritium breeder, referred to as FLIBE (Sagara et al., 2000), though a more refined FLINABE (LiF-NaF-BeF2) concept has been proposed to increase the acceptable temperature range, achieving a higher thermal efficiency (Sagara et al., 2017).

In HELIAS configurations, magnetic islands are naturally generated at the plasma edge. These islands are intersected by divertor plates forming the so-called ‘island divertor’. Successfully tested in Wendelstein 7-AS (McCormick et al., 2003) and the subject of further detailed investigations in W7-X (Niemann et al. 2020), this is a promising exhaust concept for a stellarator reactor. In the FFHR heliotron concept the divertor configuration also originates naturally from the helical geometry,

producing a continuous helical ‘double null’-like configuration. However, plasma detachment is necessary to protect the divertor against local hotspots produced by toroidal asymmetries. Selection of a favourable magnetic configuration and/or application of resonant magnetic perturbations (RMP) are options to achieve reduced heat loads (Yanagi et al., 2012). Advanced divertor concepts using molten tin shower jets or a metal pebble flow are also under investigation (Miyazawa et al., 2017, Ohgo et al., 2019).

To bridge the physics and engineering gaps between W7-X and a HELIAS reactor, several options for an intermediate-step stellarator have been proposed (Warmer et al., 2016). An intermediate device could either be: a) a physics-focused device with significant fusion power to study burning plasmas and which can also be used as a steady-state volumetric neutron source; b), a technology focused DEMO-like device, including a full prototype blanket, aiming to provide an integrated systems solution with a moderate amount of net electricity. The HELIAS line, features a high aspect ratio, but studies of more compact stellarator designs with two or three field periods are also ongoing (Henneberg et al., 2019]. Although no such device exists, a small prototype experiment is planned in China (Isobe et al., 2019). A recent study showed that it is, in principle, possible to substantially simplify the magnetic field coils of such a device by introducing additional permanent magnets that can generate a part of the poloidal flux and rotational transform (Helander et al., 2020).

For the FFHR concept, a step-by-step development strategy is considered focusing on system integration to overcome the engineering and technology challenges: 1) FFHR-a1, a device for demonstration of advanced engineering in a non-nuclear environment; 2) FFHR-b2, a steady-state neutron source for material qualification and testing, as well as providing an early demonstration of DT fusion in the stellarator configuration; 3) FFHR-c1, a heliotron DEMO; and 4) FFHR-d1, a full-scale power plant (Miyazawa et al., 2019). High-temperature superconductors are an option for these designs, allowing higher magnetic field and more compact devices.

4. Fusion Materials Test Facilities

4.1. Introduction

Radiation damage in materials is a complex function of two competing basic phenomena (nuclear reactions and elastic collisions) for the primary damage and the specific characteristics of each material components, as well as temperature, for the later evolution of the initial effects (see Litnovsky et al. (2020) for a more detailed description of reactor materials). Elastic collisions induce atomic displacement of the ions inside the materials giving rise to point defects and nuclear reactions give rise to material activation and impurification. The relative relevance of both types of reactions is a strong function of the irradiating particles, their energy and the material composition. This complexity makes it almost impossible at present to predict the behavior of materials in a radiation environment, and systematic characterization experiments are required in the future, especially for the case of high-dose irradiation conditions (Knaster et al., 2016b)

The radiation environment of a fusion reactor is also a complex function of the reactor design and it is strongly dominated by the presence of the 14 MeV neutrons produced by fusion reactions in the areas close to the first wall. This complex environment very soon raises the need for a fusion-like neutron source focused on the development and qualification of the materials to be used in a fusion reactor. This source will mainly be used during the design phase of the fusion device (in order to define the design window of the different components) and during the licensing phase (in order to demonstrate to the licensing body that the properties of the structural materials used in the fabrication of the device are sufficiently robust under nuclear conditions, to ensure that the safety of the reactor is guaranteed). Taking this into account, the requirements for the neutron source facility can be summarized as: "*the facility should be able to produce fusion-like neutrons with an intensity large enough to allow accelerated testing, up to a damage level above the expected operational lifetime in a reactor, and in an irradiation volume large and uniform enough to allow the characterization of the macroscopic properties of the materials of interest required for the engineering design of the fusion machine*". Here it is important to emphasize that the need to characterize the behavior of engineering macroscopic properties requires the use of a relatively large irradiation volume. In order to minimize this volume, the use of small sample testing techniques is nowadays strongly being developed.

The specifications of the irradiation requirements are a function of the specific fusion power plant design. In most countries with a significant fusion program, the present strategy is based on a stepped approach in which it is planned to qualify radiation effects up to the dose required by the different DEMO designs and, at a later stage, the fusion power plant needs will be addressed. So, for example, in the case of the European Roadmap and the EU-DEMO currently under development, the facility should provide a neutron flux in the high flux region of the source enabling the accumulation of fluences of 20-30 Norgett-Robinson-Torrens (NRT; Norgett et al. 1975) displacements per atom (dpa) in <2.5 years applicable to a 0.3 liter irradiation volume, and fluences of 50 NRT-dpa in <3 years applicable to a 0.1 liter volume.

It is important to note that several neutron sources are already available (e.g. materials test reactors), which are able to provide the required neutron flux. However, their energy characteristics are very different from those of a fusion reactor. Consequently, they can be of interest to study materials irradiation effects, but they are not useful for the qualification of the materials in a fusion reactor. For example, neutrons produced in fission reactors have a lower energy (typically up to 1-2 MeV) and the number of transmutation reactions will therefore be much smaller than in the case of

neutrons produced in a fusion-like environment. On the other side, the energy spectra of the neutrons produced in spallation sources have a very high-energy tail and, as a consequence, the number and type of transmutation reactions are much higher than in the case of a fusion-like environment (Zinkle and Möslang, 2013).

4.2. Fusion-like neutron sources

In recent decades, a variety of concepts have been proposed for building a neutron facility which satisfies the testing requirements discussed above. All are based either on the production of neutrons by the interaction of D and T, or on the production of neutrons by using the interaction between a light ion (usually D) and a light target (like Li, C or Be). In the latter case, the neutron spectra produced are not exactly the same as those in a fusion reactor, but the predicted effects in the materials have been assessed to be similar. The two approaches have given rise to several different proposals, although the only one currently in a relevant engineering design phase is the so-called IFMIF-DONES (International Fusion Materials Irradiation Facility- DEMO Oriented Neutron Source) project described in more detail in section 4.3.

The most obvious way to produce fusion-like neutrons is by using the D-T reaction. Usually such facilities are based on a low energy deuteron beam (a few hundreds of keV) impinging on a tritium target. The target can be solid, with tritium embedded in a solid matrix (SORGENTINA (Pillon et al., 2014), HINEG-II (Wu, 2016)) or gaseous (PNL/UW (Kulcinski et al., 2017)). The main difficulty of this approach is linked to the fact that, to obtain the required neutron flux, a high reaction rate is required. For solid targets, this is only possible with a very high power density, which is beyond present technological capabilities. Alternatively, a high number of smaller neutron sources can be applied (PNL/UW). Nevertheless, conceptual designs which have been proposed are not able to reach the required neutron fluxes.

Thus, for example, SORGENTINA is a project in which an intense 14 MeV D-T neutron source is based on continuous D and T ion beams at 40 A, 200 keV energy, impinging onto a 2 m diameter water-cooled rotating target operated at a rotational speed of about 1000 rpm. It produces up to about 10^{15} n/s (about 1×10^{13}n/cm^2 s over about 50 cm^3 and dpa rates corresponding to 2-4 dpa per full-power year (fpy)). The facility makes use of an ion source and accelerator stages from neutral beam injectors utilized at large experimental tokamaks together with a properly scaled rotating target technology.

The PNL/UW proposal is able to produce peak damage levels of ≈4–6 dpa/fpy in 15 cm^3 and has a test volume of ≈600 cm^3 covering the damage range from 1 to 6 dpa/fpy. This design is based on a quasi-commercial linear 14 MeV DT neutron source generated by injecting a 300 keV deuterium beam (of a few hundred mA intensity) into a 30 Torr tritium gas target (the pressure in the target can be tuned to optimize the irradiation parameters). A number of these small neutron sources can be arranged in a lattice configuration in which the materials to be irradiated can be located.

An interesting alternative approach is represented by the so-called "volumetric" neutron sources in which a plasma device with no energy gain (Q<1), but with external heating and an external supply of D and T is used to produce 14 MeV neutrons. The Gas Dynamic Trap (GTD) (Anikeev et al., 2015) is based on a special magnetic mirror system for plasma confinement. The main advantage of this type of neutron source is that the available irradiation volume is high (typically volumes of 0.3 liters at >15 dpa/full power year; 17.5 liters at 10-15 dpa/fpy; 6.9 liters at 5-10 dpa/fpy and 24.7 liters at <5 dpa/fpy; Fischer et al., 2000). The main difficulties are related to the plasma regime (still not fully demonstrated), the required availability (continuous operation) and all the aspects related to the

device engineering (especially tritium and remote handling management). Also some of the ST-based concepts discussed in Sec. 3.3 have been proposed as Component Test Facilities as they exhibit the proper fusion neutron spectrum (Peng et al., 2017).

The production of neutrons by using the interaction of D with other light ions in solid targets is utilised in FAFNIR (Surrey, 2014) in which a C target is used. Its performance is limited by the power handling capability of the target. Facilities in which a D-beam interacts with light ions in liquid metals constitute the IFMIF family of devices, including the IFMIF proposal (Knaster et al., 2014)], IFMIF-DONES (Ibarra et al., 2017), A-FNS (Ochiai et al., 2020) and BISOL (Liu et al., 2019)). The principle is based on Li(d,xn) nuclear reactions taking place in a liquid Li target when bombarded by a deuteron beam. To obtain neutron spectra comparable to that in the first wall of a fusion power reactor, the deuteron beam is accelerated up to 40 MeV. The main difference between the various proposals is linked to the accelerator current and, as a consequence, with the corresponding irradiation performance for each.

4.3. IFMIF-DONES

The IFMIF-DONES facility will be the neutron source that can provide conditions such as anticipated for EU-DEMO. To obtain irradiation conditions comparable to those at the first wall of a fusion power reactor, the DONES Facility will produce a 125 mA deuteron beam, accelerated up to 40 MeV (5 MW beam power) and shaped to have a footprint in the range from 100 mm x 50 mm to 200 mm x 50 mm, providing an irradiation volume of up to 0.5 l that can house around 1,000 small specimens irradiated to a high dose rate (over 10 dpa/fpy). The beam will impinge on a 25 mm thick liquid lithium target intersecting the beam with a transverse velocity of about 15 ms^{-1}. The Li(d,xn) stripping reactions will generate a large number of neutrons (up to 5×10^{18} n/m^2s) that will interact with the material samples located immediately behind the lithium target, in the Test Modules (Ibarra et al., 2018).

The site-specific engineering design of the IFMIF-DONES facility has been underway since 2015 with the objective to be ready for construction of the facility in the early 2020´s (Ibarra et al., 2019) in Granada (Spain). It is based on the IFMIF engineering design (Knaster et al., 2015) developed in the framework of the IFMIF/EVEDA (acronym that stands for Engineering Validation and Engineering Design Activities) project, but updated to take into account the validation results obtained plus modelling calculations, and simplified as much as possible in order to reduce cost. Figure 9 shows a schematic view of the operational principles and a simplified CAD drawing of the facility.

The IFMIF/EVEDA project also developed a number of prototyping sub-projects (Knaster et al., 2013), including: i) an Accelerator Prototype (LIPAc), assembling IFMIF components up to its first superconducting acceleration stage (9 MeV energy, 125 mA of D^+ continuous wave current); and ii) the EVEDA experimental Lithium Test Loop (ELTL), which integrated all elements of the IFMIF Li target facility that was used to test the long-time stability of the liquid lithium jet forming the target. Results obtained to date have not identified any significant showstoppers.

Taking all these results into account, the construction phase of IFMIF-DONES could start in the early 2020's and the facility could be operational around ten years later. The aim is to produce first preliminary data around 2035, on time for the engineering design of EU-DEMO.

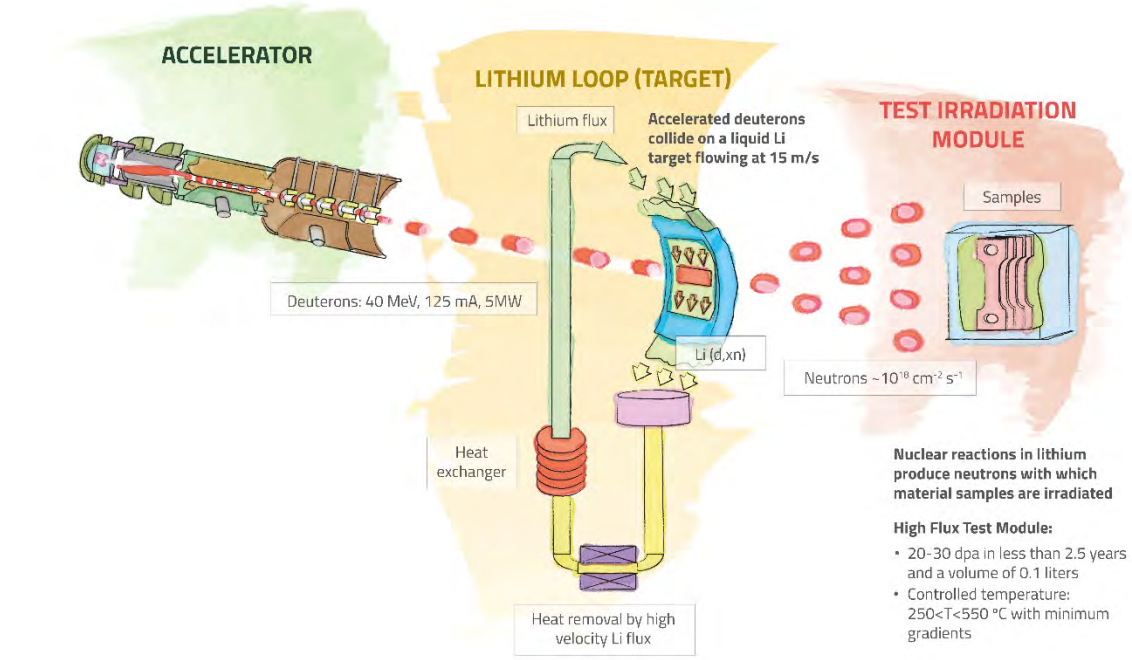

Figure 9. IFMIF-DONES facility: (a) Schematic view of the operational principles, (b) a simplified CAD drawing

5. Non-nuclear development facilities

Several significant non-nuclear development facilities are currently under construction, or in planning, which are expected to deliver important complementary R&D information to the nuclear devices described in earlier sections. All of these devices are non-nuclear in the sense that they will not operate with a deuterium-tritium mixture.

	COMPASS-U	DTT	HL-2M	JT-60SA
Major Radius (m)	0.84	2.10	1.78	2.96
Minor Radius (m)	0.28	0.65	0.65	1.18
Toroidal Field (T)	5.0	6.0	2.2	2.25
Plasma Current (MA)	2.0	5.5	2.5	5.5
ECRH (MW)	4	20	2 (4)	7
ICRF (MW)		15		
NBH (MW)	4-5	- (10)	2 (4)	34
LHH (MW)			- (2)	
Expected operation	Late 2021	2025	Late 2020	Late 2020

The largest of these devices is the Japanese-European JT-60SA tokamak (Barabaschi et al., 2019). The mission of JT-60SA is to contribute to the early realization of fusion energy by addressing key physics issues for ITER and DEMO. It is a fully superconducting tokamak capable of confining high-temperature (100 million degree) deuterium plasmas, under plasma conditions equivalent to 'breakeven' (where the fusion power would be equal to the input power if the plasma were operated in D-T). It is designed to support the optimization of the plasma configurations for ITER and DEMO and has a high plasma heating and current drive power, using both positive and negative ion based neutral beams, as well as ECRH. It will typically operate for 100 s pulses once per hour, subjecting water-cooled divertors to maximum heat fluxes of 15 MWm^{-2}. The device will be able to explore fully non-inductive steady-state operation. The assembly of JT-60SA was completed in 2020 and, on entry into operation in spring 2021, it will be the world's largest operating tokamak, in succession to the Joint European Torus.

COMPASS-U in Prague (Panek et al., 2017) is a high field, high-density tokamak, with a flexible set of poloidal field coils for generation of single-null, double-null and snowflake divertor configurations. In addition, COMPASS-U will be equipped with a closed divertor operated at high plasma and neutral density and with high optical opacity similar to future reactors. COMPASS-U will address some of the key challenges in the field of the plasma exhaust physics, reactor-relevant edge plasma physics, advanced confinement regimes, advanced magnetic configurations and materials for next-step devices. The copper coils are cooled with liquid nitrogen to allow for higher magnetic fields.

The Divertor Test Tokamak in Frascati (Albanese et al., 2019) is a high-field superconducting tokamak aimed at exploring and qualifying alternative power exhaust solutions for DEMO. The device will have the possibility to test several different magnetic divertor topologies in relevant reactor regimes. Various plasma facing materials will be tested (e.g. tungsten, liquid metals) at divertor heat fluxes in excess of 20 MWm^{-2}. The final target of the experiment is the realization of an integrated solution (bulk and edge plasma) for the power exhaust in view of DEMO. For this purpose, the DTT tokamak has edge conditions that are similar to those of DEMO in terms of dimensionless parameters.

HL-2M (Li et al., 2015) is a copper-conductor tokamak under construction in Chengdu, China and is dedicated to studying the critical physics and engineering issues of ITER and CFETR.

Acknowledgement

The authors would like to thank S.J. Yoo, J. Li and Y. Sakamoto for providing and checking the data in Table 3 on K-DEMO, CFETR and JA-DEMO, respectively. The work of four of the authors (AJHD, GF, AI and FW) has been carried out within the framework of the EUROfusion Consortium and has received funding from the Euratom research and training programme 2014-2020 under grant agreement No 633053. The views and opinions expressed herein do not necessarily reflect those of the European Commission.

References

Albanese, R., Crisanti, F., Martin, P., *et al.,* 2019, Design review for the Italian Divertor Tokamak Test facility, Fusion Eng. Des. **146A** 194-197, https://doi.org/10.1016/j.fusengdes.2018.12.016.

Anikeev, A.V., Bagryansky, P.A., Beklemishev, A.D., *et al.,* 2015, Progress in Mirror-Based Fusion Neutron Source Development, Materials **8** 8452–8459; https://doi.org/10.3390/ma8125471.

Aymar, R., Barabaschi, P. and Shimomura, Y., 2002, The ITER Design, Plasma Phys. and Contr. Fusion **44**, 519-565, https://doi.org/10.1088/0741-3335/44/5/304.

Barabaschi, P., Kamada, Y., Shirai, H. and the JT-60SA Integrated Project Team, 2019, Progress of the JT-60SA project, Nucl. Fusion **59**, 112005, Progress of the JT-60SA project, https://doi.org/10.1088/1741-4326/ab03f6.

Beaumont, B., Agarwal, R., Montemayor, T.A., et al*.,* 2017, Status of the ITER Ion Cyclotron H&CD, EPJ Web Conf. **157**, 02002, https://doi.org/10.1051/epjconf/201715702002.

Bhardwaj, A.K., Gupta, G., Prajapati, R., *et al.,* 2016, Overview and status of ITER cryostat manufacturing, Fusion Eng. Des. **109-111b**, 1351-1355, https://doi.org/10.1016/j.fusengdes.2015.12.028.

Bigot, B., 2019, Progress towards ITER's first plasma, Nucl. Fusion **59**, 112001, https://doi.org/10.1088/1741-4326/ab0f84.

Boccaccini, L., et al*.,* 2020, Magnetic Confinement Fusion – Reactor Blanket Technologies, Chapter 01215.

Campbell, D.J., Akiyama, T., Barnsley, R., *et al.,* 2019, Innovations in Technology and Science R&D for ITER, J. Fusion Energy **38**, 11-71, https://doi.org/10.1007/s10894-018-0187-9.

Chapman, I.T, Adamek, J., Akers, R.J., *et al.,* 2015, Overview of MAST results, Nucl. Fusion **55** 104008, https://doi.org/10.1088/0029-5515/55/10/104008.

Chuyanov, V.A. and Gryaznevich, M.P., 2017, Modular fusion power plant, Fus. Eng. Des. **122**, 238-252, https://doi.org/10.1016/j.fusengdes.2017.07.017.

Claessens, M., 2020, ITER: The giant fusion reactor, Springer, Germany, ISBN 978-3-030-27581-5.

Damiani, C., Palmer, J. Takeda, N., *et al.,* 2018, Overview of the ITER remote maintenance design and of the development activities in Europe, Fus. Eng. Des. **136B**, 1117-1124, https://doi.org/10.1016/j.fusengdes.2018.04.085.

Darbos, C., Albajar, F., Bonicelli, T., *et al.,* 2016, Status of the ITER Electron Cyclotron Heating and Current Drive system, J. Infrared Milli TeraHz Waves **37**, 4-20, https://doi.org/10.1007/s10762-015-0211-3.

Day, C., Murdoch, D. and Pearce, R., 2008, The vacuum systems of ITER, Vacuum **83**, 773-778, https://doi.org/10.1016/j.vacuum.2008.05.010.

Dean, S.O., Baker, C.C., Cohn, D.R. and Kinkead S.D., 1991, An accelerated fusion power development plan, J. Fusion Energy **10**, 197–206, http://dx.doi.org/10.1088/0029-5515/45/2/004.

Dean, S.O., Baker, C.C., Cohn, D.R., *et al.,* 1992, Pilot plant: An affordable step toward fusion power. J Fusion Energ **11**, 85–97, https://doi.org/10.1007/BF01080171.

Devred, A., Backbier, I., Bessette, D., *et al.,* 2014, Challenges and status of ITER conductor production, Supercond. Sci. Technol. 27, 044001, http://dx.doi.org/10.1088/0953-2048/27/4/044001.

Donné, A.J.H., Costley, A.E., Barnsley, R., *et al.,* 2007, Diagnostics, Nucl. Fusion. **47**, S337-S384, https://doi.org/10.1088/0029-5515/47/6/S07.

Donné, A.J.H., Morris, A.W., *et al.,* 2018, European Research Roadmap to the Realisation of Fusion Energy, EUROfusion, Germany, ISBN 978-3-00-066152-0, https://www.euro-fusion.org/eurofusion/roadmap/.

Federici ,G., Bachmann, C., Biel, W., *et al.,* 2016 , Overview of the design approach and prioritization of R&D activities towards an EU DEMO, Fus. Eng. Des. **109–111B**, 1464–1474, https://doi.org/10.1016/j.fusengdes.2015.11.050.

Federici, G., Biel, W., Gilbert, M.R., *et al.,* 2017, European DEMO design strategy and consequences for materials, Nucl. Fusion **57**, 092002, https://doi.org/10.1088/1741-4326/57/9/092002.

Federici, G., Bachmann, C., Barucca, L., *et al.,* 2018, DEMO design activity in Europe: Progress and updates, Fusion Eng. Des. **136A**, 729-741, https://doi.org/10.1016/j.fusengdes.2018.04.001.

Federici, G., Bachmann, C., Barucca, L., *et al.,* 2019, Overview of the DEMO design-staged approach in Europe, Nucl. Fusion **59**, 066013, https://doi.org/10.1088/1741-4326/ab1178.

Federici, G*., Bachmann, C., Corato, V., Jimenez, S., You, J.H.,* 2020, Magnetic Confinement Fusion – Technology: 'Fusion Core', Chapter 01213.

Fischer, U., Möslang, A., and Ivanov A.A., 2000, Assessment of the gas dynamic trap mirror facility as intense neutron source for fusion material test irradiations, Fus. Eng. Des. **48**, 307-325, https://doi.org/10.1016/S0920-3796(00)00164-2.

Friconneau, J.-P., Beaudoin, V., Dammann, A., *et al.,* 2017, ITER hot cell – Remote handling system maintenance overview, Fusion Eng. Des. **124**, 673-676, https://doi.org/10.1016/j.fusengdes.2017.01.005.

Gates, D.A., Boozer, A.H. Brown, T., *et al.,* 2017, Recent advances in stellarator optimization Nucl. Fusion **57**, 126064, https://doi.org/10.1088/1741-4326/aa8ba0.

Giancarli, L.M., Ahn, M.-Y., Bonnett, I., *et al.,* 2018, ITER TBM program and associated system engineering, Fus. Eng. Des. **136B**, 815-821, https://doi.org/10.1016/j.fusengdes.2018.04.014.

Greenwald, M., Terry J.L., Wolfe S.M., *et al.*, 1988, A new look at density limits in tokamaks, Nucl. Fusion **28**, 2199, https://doi.org/10.1088/0029-5515/28/12/009.

Grieger, G., Lotz, W., Merkel, P., et al., 1992, Physics optimization of stellarators, Phys. Fluids, **B4**, 2081, https://doi.org/10.1063/1.860481.

Grieger, G. and Milch, I., 1993, Das Fusionsexperiment Wendelstein 7-X (in German), Physikalische Blätter **49**, 1001.

Häussle,r A., Warmer, F and Fischer, U., 2018, Neutronic analyses for a stellarator power reactor based on the HELIAS concepot, Fus. Eng. Des, **136**, 345-349, https://doi.org/10.1016/j.fusengdes.2018.02.026.

Helander, P., Drevlak, M., Zarnstorff, M. and Cowley S.C., 2020, Stellarators with permanent magnets, Phys. Rev. Lett. **124**, 095001, https://doi.org/10.1103/PhysRevLett.124.095001.

Hemsworth, R.S., Boilson, D., Blatchford, P., *et al.,* 2017, Overview of the design of the ITER heating neutral beam injectors, New J. Phys. **19**, 025005, https://doi.org/10.1088/1367-2630/19/2/025005.

Henneberg, S.A., Drevlak, M., Nührenberg, C., *et al.,* 2019, Properties of a new quasi-axisymmetric configuration, Nucl. Fusion **59**, 026014, https://doi.org/10.1088/1741-4326/aaf604.

Ibarra, A., Heidinger, R., Barabaschi, P., *et al.,* 2017, A stepped Approach from IFMIF/EVEDA toward IFMIF, Fusion Sci. Tech. **66**, 252–259, https://doi.org/10.13182/FST13-778.

Ibarra, A., Arbeiter, F., Bernardi, D., *et al.,* 2018, The IFMIF-DONES project: preliminary engineering design, Nucl. Fusion **58**, 105002, https://doi.org/10.1088/1741-4326/aad91f.

Ibarra, A., Arbeiter, F., Bernardi, D., *et al.,* 2019, The European approach to the fusion-like neutron source: the IFMIF-DONES project, Nucl. Fusion **59,** 065002, https://doi.org/10.1088/1741-4326/ab0d57.

Iiyoshi, A., Komoro, A., Ejiri, A., *et al.,* 1999, Overview of the Large Helical Device project,Nucl. Fusion **39**, 1245, https://doi.org/10.1088/0029-5515/39/9Y/313.

Ikeda, K., 2010, ITER on the road to fusion energy, Nucl. Fusion **50**, 014002, https://doi:10.1088/0029-5515/50/1/014002.

Inoue, T., *et al.,* 2020, Magnetic Confinement Fusion – Technology: Plasma Engineering, Chapter 01214.

Isobe, M., Shimizu, A., Liu, H., *et al.,* 2019, Current Status of NIFS-SWJTU Joint Project for Quasi-Axisymmetric Stellarator CFQS, Plasma and Fusion Research **14**, 3402074, https://doi.org/10.1585/pfr.14.3402074.

ITER, 2002, ITER Technical Basis, ITER EDA Documentation Series No. 24, IAEA, Vienna.

ITER Organization, 2018, ITER Research Plan within the staged approach (Level III – Provisional Version), ITER Report ITR-18-003.

Joffrin, E., Abduallev, S., Abhangi, M., *et al.,* 2019, Overview of the JET preparation for deuterium-tritium operation with the ITER-like wall, Nucl. Fusion **59**, 102872, https://doi.org/10.1088/1741-4326/ab2276.

Kang J.S., Park J.M., Jung L., et al., 2017, Development of a systematic, self-consistent algorithm for the K-DEMO steady-state operation scenario, Nucl. Fusion **57**, 126034, https://doi.org/10.1088/1741-4326/aa7072.

Kemp, R., Wenninger, R., Federici, G., *et al.,* 2018, Exploring a broad spectrum of design options for DEMO, Fus. Eng. Des. **136**, 970-974, https://doi.org/10.1016/j.fusengdes.2018.04.049.

Kessel, C.E., Blanchard, J.P., Davis, A., *et al.,* 2018, Overview of the fusion nuclear science facility, a credible break-in step on the path to fusion energy, Fusion Eng. Des. **135B**, 236-270, https://doi.org/10.1016/j.fusengdes.2017.05.081.

Kim, K., Im, K., Kim, H.C., *et al.,* 2015, Design concept of K-DEMO for near-term implementation, Nucl. Fusion **55**, 053027, http://dx.doi.org/10.1088/0029-5515/55/5/053027.

Knaster, J., Arbeiter, F., Cara, P., *et al.,* 2013, IFMIF: overview of the validation activities, Nucl. Fusion **53**, 116001, http://dx.doi.org/10.1088/0029-5515/53/11/116001.

Knaster, J., Ibarra, A., Abal, J., *et al.,* 2015, The accomplishment of the Engineering Design Activities of IFMIF/EVEDA: the European-Japanese project towards a Li(d,xn) fusion relevant neutron source. Nucl. Fusion **55**, 086003, https://doi.org/10.1088/0029-5515/55/8/086003.

Knaster, J., Arbeiter, F., Cara, P., *et al.,* 2016a, IFMIF, a fusion relevant neutron source for material irradiation current status, J. Nucl. Mater. **453**, 115-119, https://doi.org/10.1016/j.nme.2016.04.012.

Knaster, J., Moeslang, A. and Muroga, T., 2016b, Materials research for fusion, Nature Phys. **12**, 424–434, https://doi.org/10.1038/nphys3735

Knaster, J., Garin,, P., Matsumoto, H., *et al.,* 2017, Overview of the IFMIF/EVEDA project, Nucl. Fusion **57**, 102016, https://doi.org/10.1088/1741-4326/aa6a6a.

Kovari, M., Kemp, R., Lux, H., *et al.,* 2014, "PROCESS": A systems code for fusion power plants—Part 1: Physics, Fus. Eng. Des. **89**, 3054-3059, https://doi.org/10.1016/j.fusengdes.2014.09.018.

Kovari, M., Fox, F., Harrington, C., *et al.,* 2016, "PROCESS": A systems code for fusion power plants – Part 2: Engineering, Fus. Eng. Des. **104**, 9-20, https://doi.org/10.1016/j.fusengdes.2016.01.007.

Kuang, A.Q., Cao, N.M., Creely A.J. *et al.,* 2018, Conceptual design study for heat exhaust management in the ARC fusion pilot plant, Fus. Eng. Des. **137**, 221-242, https://doi.org/10.1016/j.fusengdes.2018.09.007.

Kulcinski, G.L., Radel, R.F and Davis, A., 2017, An Improved Near Term 14 MeV Neutron Test Facility for Fusion Power Plant Materials, Fusion Sci. Tech. **72,** 248-254, https://doi.org/10.1080/15361055.2017.1333861.

Kumar, A.G.A., Gupta, D.K., Patel, N., *et al.,* 2013, Preliminary design of ITER component cooling water system and heat rejection system, IEEE 25th Symposium on Fusion Engineering (SOFE), San Francisco, CA, 2013, pp. 1-5, doi: 10.1109/SOFE.2013.6635383.

Lao, L., *et al.,* 2020, Magnetic Confinement Fusion - Plasma Theory: Magnetohydrodynamic Stability, Chapter 01206

Lehnen, M., Aleynikova, K., Aleynikov, P.B., *et al.,* 2015, Disruptions in ITER and strategies for their control and mitigation, J. Nucl. Mat. **463**, 39-48, https://doi.org/10.1016/j.jnucmat.2014.10.075.

Li, Q., and HL-2M Team, 2015, The component development status of HL-2M tokamak, Fus. Eng. Des. **96-97**, 338-342, https://doi.org/10.1016/j.fusengdes.2015.06.106.

Lioce, D., Orlandi, S., Moteleb, M., *et al.,* 2019, ITER Tokamak Colling Water System Design, Fus. Sci. Techn. **75**, 841-848, https://doi.org/10.1080/15361055.2019.1644135.

Litnovsky, A., et al., 2020, Magnetic Confinement Fusion – Reactor Materials, Chapter 01216.

Liu, Q., Yan, S., Hu, Y., *et al.,* 2019, BISOL The preliminary conceptual design of the high-power neutron converter for BISOL, Nucl. Instrum. Meth. Phys. B **456**, 108-115, https://doi.org/10.1016/j.nimb.2019.07.012.

Martin, Y., Takizuka, T., *and ITPA CDBM H-Mode Threshold Database Working Group*, 2008, Power requirement for accessing the H-mode in ITER, Journal of Physics: Conf. Series, **123**, 012033, https://doi.org/10.1088/1742-6596/123/1/012033.

Martinez, J.-M., Alekseev, A., Sborchia, C., *et al.,* 2016, ITER vacuum vessel structural analysis completion during manufacturing phase, Fusion Eng. Des. **109-111**, 688-692, https://doi.org/10.1016/j.fusengdes.2016.02.017.

McCormick, K., Grigull, P., Burhann, R., *et al.,* 2003, Island divertor experiments on the Wendelstein 7-AS stellarator, J. Nucl. Mat. **313-316**, 1131, https://doi.org/10.1016/S0022-3115(02)01506-4.

Menard, J.E., Bromberg, L., Brown, T., *et al.,* 2011, Prospects for pilot plants based on the tokamak, spherical tokamak and stellarator, Nucl. Fusion **51**, 103014, https://doi.org/10.1088/0029-5515/51/10/103014.

Menard, J.E., Gerhardt, S., Bell, M., *et al.,* 2012, Overview of the physics and engineering design of NSTX upgrade, Nucl. Fusion **52**, 083015, https://doi.org/10.1088/0029-5515/52/8/083015.

Menard, J.E., Brown, T., El-Guebaly, L., *et al.,* 2016, Fusion nuclear science facilities and pilot plants based on the spherical tokamak, Nucl. Fusion **56**, 106023, https://doi.org/10.1088/0029-5515/56/10/106023.

Menard, J.E., 2019, Compact steady-state tokamak performance dependence on magnet and core physics limits, Phil. Trans. R. Soc. A **377:** 20170440. http://dx.doi.org/10.1098/rsta.2017.0440

MFE16, 2016, Magnetic Fusion Energy: From Experiments to Power Plants. Chapter 19: Stellarator fusion power plants. A volume in the Woodhead Publishing Series in Energy (2016).

Mitchell, N. and Devred, A., 2017, The ITER magnet system: configuration and construction status, Fusion Eng. Des. **123**, 17, http://dx.doi.org/10.1016/j.fusengdes.2017.02.085.

J. Miyazawa, Goto, T., Murase, T., *et al.,* 2017, Conceptual design of a liquid metal limiter/divertor system for the FFHR-d1, Fus. Eng. Des. **125**, 227-238, https://doi.org/10.1016/j.fusengdes.2017.07.003.

J. Miyazawa, Goto T., Tamura T., *et al.,* 2019, The strategy toward realization of the helical fusion reactor FFHR-c1, Fus. Eng. Des. **146B**, 2233-2237, https://doi.org/10.1016/j.fusengdes.2019.03.160.

Monneret, E., Benkheira, L., Fauve E., *et al.,* 2017, ITER cryoplant final design and construction, IOP Copnf. Series: Mat. Sci. Eng. **171**, 012031, http://dx.doi.org/10.1088/1757-899X/171/1/012031.

National Academy of Sciences, Engineering and Medicine, 2019, Final Report of the Committee on a Strategic Plan for U.S. Burning Plasma Research, The National Academies Press, Washington, DC. ISBN: 978-0-309-48743-6, https://doi.org/10.17226/25331.

Neilson G.H., Brown T., Im K., *et al.,* 2014, Physics and engineering assessments of the K-DEMO magnet configuration, Proc. 25th Fusion Energy Conference, Saint Petersburg, Russia, 13-18 October 2014, paper FIP/P7-2.

Neumeyer, C., Benfatto, I., Hourtoule, J., *et al.,* 2013, ITER power supply innovations and advances, IEEE 25th Symposium on Fusion Engineering (SOFE), San Francisco, CA, 2013, pp. 1-8, doi: 10.1109/SOFE.2013.6635287.

Niemann, H., Drewelow, P., Jakubowski, M.W., *et al.,* 2020, Large wetted areas of divertor power loads at Wendelstein 7-X, Nucl. Fusion, **60**, 084003, https://doi.org/10.1088/1741-4326/ab937a.

Norgett, M.J., Robinson, M.T. and Torrens, I.M., 1975, A proposed method of calculating displacement dose rates, Nucl. Eng. and Design, **33**, 50-54,

Ochiai, K., Sato, S., Kondo, H., *et al.,* 2020, Conceptual design progress of Advanced Neutron Source, Nucl. Fusion in press, https://doi.org/10.1088/1741-4326/ab9125.

Ohgo, T., Goto, T. and Miyazawa, J., 2019, A New Divertor System Using Fusible Metal Pebbles, Plasma Fusion Res. **14**, 3405050, https://doi.org/10.1585/pfr.14.3405050.

Okano, K., 2019, Review of Strategy Toward DEMO in Japan and Required Innovations, J. Fusion Ener. **38**, 138-146, https://doi.org/10.1007/s10894-018-0169-y.

Panek, R., Markovic, T., Cahyna, P., *et al.,* 2017, Overview of the COMPASS upgrade tokamak, Fus. Eng. Des. **123**, 11-16, https://doi.org/10.1016/j.fusengdes.2017.03.002.

Peng, Y.K.M., Burgess, T.W., Carroll, A.J., *et al.,* 2009, Remote Handling and Plasma Conditions to Enable Fusion Nuclear Science R&D Using a Component Testing Facility, Fusion Sci. and Tech., **56**, 957-964, https://doi.org/10.13182/FST09-A9034.

Pillon, M., Angelone, M., Pizzuto, A. and Pietropaolo,, A., 2014, Feasibility study of an intense D-T fusion source: "The new sorgentina", Fusion Eng. Des. **89**, 2141 – 2144, https://doi.org/10.1016/j.fusengdes.2014.01.058.

Reux, C., Kahn, S., Zani, L., *et al.,* 2018, DEMO design using the SYCOMORE system code: Influence of technological constraints on the reactor performances, Fus. Eng. Des. **136**, 1572-1576, https://doi.org/10.1016/j.fusengdes.2018.05.059.

Rosanvallon, S., Torcy, D., Chon, J.K. and Dammann, A., 2016, Waste management plans for ITER, Fusion Eng. Des. **109-111B**, 1442-1446, https://doi.org/10.1016/j.fusengdes.2015.12.002.

Sagara, A., Yamanishi, H., Imagawa, S., *et al.,* 2000, Design and development of the Flibe blanket for helical-type fusion reactor FFHR, Fus. Eng. Des. **49**, 661-666, https://doi.org/10.1016/S0920-3796(00)00360-4.

Sagara, A., Goto, T., Miyazawa, J., *et al.,* 2012, Design activities on helical DEMO reactor FFHR-d1, Fus. Eng. Des. 87, 594, https://doi.org/10.1016/j.fusengdes.2012.01.030.

Sagara, A., Miyazawa, J., Tamura, H., *et al.,* 2017, Two conceptual designs of helical fusion reactor FFHR-d1A based on ITER technologies and challenging ideas, Nucl. Fusion **57**, 086046, https://doi.org/10.1088/1741-4326/aa6b12.

Schauer, F., Egorov, K. and Bykov, V., 2011, Coil winding pack FE-analysis for a HELIAS reactor, Fusion Eng. Des. **86**, 636-639, https://doi.org/10.1016/j.fusengdes.2011.01.058.

Schauer, F., Egorov, K. and Bykov, V., 2013, HELIAS 5-B magnet system structure and maintenance concept, Fusion Eng. Des. **88**, 1619-1622, https://doi.org/10.1016/j.fusengdes.2013.01.035.

Sekachev, I., Meekins, M., Sborchia, C., *et al.,* 2015, The Cryostat and Subsystems Development at ITER, Phys. Procedia **67**, 294-301, https://doi.org/10.1016/j.phpro.2015.06.090.

Shimomura, Y. for the ITER Central Team and Home Teams, 2001, ITER Technology R&D, Fusion Eng. Des. **55**, 97 (special issue devoted to ITER Technology R&D)

Siccinio, M., Federici, G., Kembleton, R., *et al.,* 2019, Figure of merit for the divertor protection in the preliminary design of the EU-DEMO reactor, Nucl. Fusion **59**, 106026 https://doi.org/10.1088/1741-4326/ab3153.

Singh, M.J., 2016, Status of heating and current drive systems planned for ITER, IEEE Transact. Plasma Sci. **44**, 1514-1524, https://doi.org/10.1109/TPS.2016.2577709.

Snipes, J.A., Albanese, R., Ambrosino, G., *et al.,* 2019, Overview of the preliminary design of the ITER plasma control system, Nucl. Fusion **59**, 125001, https://doi.org/10.1088/1741-4326/aa8177.

Song, X.M., Li, J.X., Leuer, J.A., Zhang, J.H. and Song, X., 2019, First plasma scenario development for HL-2M, Fusion Eng. Des. **147**, 111254, https://doi.org/10.1016/j.fusengdes.2019.111254.

Sorbom, B.N., Ball, J., Palmer, T.R., *et al.,* 2015, ARC: A compact, high-field, fusion nuclear science facility and demonstration power plant with demountable magnets, Fusion Eng. Des. **100**, 378-405, https://doi.org/10.1016/j.fusengdes.2015.07.008.

Strait, E.J., Barr, J.L, Baruzzo, M., *et al.,* 2019, Progress in disruption prevention for ITER, Nucl. Fusion **59**, 112012, https://doi.org/10.1088/1741-4326/ab15de.

Surrey, E., Porton, M., Caballero, A., *et al.,* 2014, FAFNIR: strategy and risk reduction in accelerator driven neutron sources for fusion materials irradiation data, Fusion Eng. Des. **89**, 2108–2113 (2014), http://dx.doi.org/10.1016/j.fusengdes.2014.03.042.

Sykes, A., Costley, A.E., Windsor, C.G., *et al.,* 2018, Compact fusion energy based on the spherical tokamak, Nucl. Fusion **58**, 016039, https://doi.org/10.1088/1741-4326/aa8c8d.

Tamura H., Tanaka T., Goto T. *et al.*, 2015, Fusion Eng. Des. **98–99**, 1629-1633, https://doi.org/10.1016/j.fusengdes.2015.01.025.

Taylor, N., Alejaldre, C., Cortes, P., 2013, Progress in the safety and licensing of ITER, Fusion Sci. Techn. **64**, 111-117, https://doi.org/10.13182/FST13-A18064.

Tobita, K., Hiwatari, R., Sakamoto, Y., *et al.,* 2019, Japan's efforts to develop the concept of JA DEMO during the past decade, Fusion Sci. Techn. **75**, 372-383, https://doi.org/10.1080/15361055.2019.1600931.

Vostner, A., Bontemps, V., Encheva, A., *et al.,* 2019, The ITER In-Vessel Coils – design finalization and challenges, Fusion Eng. Des. **146B**, 1490-1495, https://doi.org/10.1016/j.fusengdes.2019.02.113.

Walsh, M., Andrew, P., Barnsley, R., *et al.,* 2015, Integration of Diagnostics on ITER, Proc. IEEE 26th Symposium on Fusion Engineering (SOFE), https://doi.org/10.1109/SOFE.2015.7482260.

Wan, Y., Li., J., Liu, Y., *et al.,* 2017, Overview of the present progress and activities on the CFETR, Nucl. Fusion **57**, 102009, https://doi.org/10.1088/1741-4326/aa686a.

Warmer, F., Beidler, C.D., Dinklage, A., Wolf, R., and the W7-X Team, 2016, From W7-X to a HELIAS fusion power plant: motivation and options for an intermediate-step burning-plasma stellarator, Plasma Phys. Control. Fusion, **58**, 074006, https://doi.org/10.1088/0741-3335/58/7/074006.

Wenninger, R., Kemp, R., Maviglia, F., *et al.,* 2015, DEMO Exhaust Challenges Beyond ITER, Proc. of the 42nd EPS Conference on Plasma Physics, 22 – 26 June 2015, Lisbon, Portugal – EUROfusion, p 4.110.

Wigram, M.R.K., LaBombard, B., Umansky, M.V., *et al.,* 2019, Performance assessment of long-legged tightly-baffled divertor geometries in the ARC reactor concept, Nucl. Fusion **59**, 106052, https://doi.org/10.1088/1741-4326/ab394f.

Wilson, H.R., 2020, STEP – On the Pathway to Fusion Commercialisation, published in 'Commercialising Fusion - How small businesses are transforming big science' by IAEA.

Windridge, M., 2019, Smaller and quicker with spherical tokamaks and high-temperature superconductors, Phil. Trans. R. Soc. A**377**, 20170438, http://dx.doi.org/10.1098/rsta.2017.0438.

Wu, Yu., 2016, Development of high intensity D–T fusion neutron generator HINEG, Int. J. Energy Res. **42**, 68–72, https://doi.org/10.1002/er.3572.

Yamada, H., 2020, Magnetic Confinement Fusion – Experimental Physics, Stellarators, Chapter 01211.

Yanagi, N., Ito, S., Terazaki, Y., et al., 2015, Design and development of high-temperature superconducting magnet system with joint-winding for the helical fusion reactor, Nucl. Fusion **55**, 053021, https://doi.org/10.1088/0029-5515/55/5/053021.

Yanagi, N., Goto, T., Miyazawa, J., *et al.,* 2019, Progress in the Conceptual Design of the Helical Fusion Reactor FFHR-d1, J. Fusion Ener. **38**, 147-161, https://doi.org/10.1007/s10894-018-0193-y.

Zhuang, G., Li G.Q., Li J., *et al.,* 2019, Progress of the CFETR design, Nucl. Fusion **59,** 112010, https://doi.org/10.1088/1741-4326/ab0e27.

Zinkle, S. and Möslang, A., 2013, Evaluation of irradiation facility options for fusion materials research and development, Fusion Eng. Des. **88**, 472–482, https://doi.org/10.1016/j.fusengdes.2013.02.081.

Zohm, H., 2020, Magnetic Confinement Fusion - Experimental Physics: Tokamaks, Chapter 01210